Austrian Journal of Earth Sciences | Vienna | 2015 | Volume 108/2 | 151 - 171 | DOI: 10.17738/ajes.2015.0018

The Trattnach Oil Field in the North Alpine Foreland Basin (Austria)

Doris GROSS[1)*)], Reinhard SACHSENHOFER[1)], Arno RECH[1)3)], Stefan SAGEDER[1)4)], Martin GEISSLER[1)2)], Stephan SCHNITZER[1)5)] & Wilma TROISS[2)]

[1)] Chair of Petroleum Geology, Department Applied Geosciences and Geophysics, Montanuniversität Leoben, Peter-Tunner-Strasse 5, 8700 Leoben, Austria;

[2)] Rohöl-Aufsuchungs AG, Schwarzenbergplatz 16, 1015 Wien, Austria;

[3)] OMV AG, 2230 Gänserndorf, Austria;

[4)] Total E&P, 64018 Pau, France;

[5)] GDF SUEZ E&P Deutschland GmbH, Waldstraße 39, 49803 Lingen, Germany;

[*)] Corresponding author, doris.gross@unileoben.ac.at

KEYWORDS Cenomanian green sandstones; Trattnach Anticline; Alpine Foreland Basin; Upper Austria

Abstract

The Trattnach Field, located in the Upper Austrian part of the North Alpine Foreland Basin produces oil from a depth of about 1600 m since the 1970s. Within an industry-university cooperation RAG provided drill cores, geological and geophysical data, including a 70 km^2 seismic cube, to Montanuniversität Leoben. Results of several studies based on this data set are summarized in the present paper.

Sedimentation in the Trattnach area commenced during Jurassic time with clastic sediments and platform carbonates. The latter became karstified during the Early Cretaceous. Non-marine sediments (Schutzfels Formation) filled karst structures. Shallow marine Cenomanian sediments (Regensburg Formation), about 30 m thick, overlie Schutzfels Formation or Jurassic carbonates and often start with a transgressive conglomerate. The dominant lithology is highly bioturbated glauconite rich sandstone. A reddish conglomerate ("marker bed") and calcareous sandstones occur in the upper part. Tempestites and debris flows are frequent. Turonian calcareous shales (Eibrunn Formation) overlie the Cenomanian sediments.

The oldest structural elements visible in the Trattnach 3D cube are related to Turonian/Coniacian E-W compression, a consequence of the opening of the N-Atlantic. Paleocene NE-SW compression, related to the closure of the Penninic Ocean, caused the formation of the Trattnach Mega-Anticline and transpressional reactivation of the NNW-SSE trending late Variscan Schwanenstadt fault system.

Eocene clastic and carbonate rocks overlie the Mesozoic succession with an angular unconformity. Fine-grained rocks follow above the Eocene carbonates. Locally, these sediments were removed by extensive Lower Oligocene submarine slides. Another unconformity separates the Upper Puchkirchen Formation (Egerian) from the Hall Formation (Eggenburgian).

E-W trending normal faulting (Aistersheim and Gaspoltshofen fault systems) related to flexural down-bending is the main Cenozoic tectonic event. Both fault systems were activated during earliest Oligocene time. Fault activity decreased during Egerian time and ended before the Eggenburgian. Seismic data provide evidence for rotation of the fault block confined by the Aistersheim and Gaspoltshofen faults during late Oligocene (early Egerian) time.

The Trattnach Field is located within the Trattnach Anticlinal Dome. Its western boundary is formed by the Schwanenstadt fault system. The Trattnach Field produces oil from the lower part of the Cenomanian green sandstones (CE3, CE2). Reservoir quality is controlled by grain size, clay mineral and carbonate cement. The seal is formed by Cenomanian rocks with low permeability (CE1) and Turonian calcareous shales. The Trattnach oil has low sulfur content and is undersaturated with respect to gas. Oil accumulation commenced during Miocene time. Oil field water with low salinity indicates a hydraulic connection with meteoric water within Jurassic carbonate rocks.

Das Trattnach-Feld befindet sich in der oberösterreichischen Molassezone und produziert seit den 1970er Jahren Öl aus einer Tiefe von ca. 1600 m. Im Rahmen einer Industrie-Universitäts-Kooperation hat die Firma RAG Bohrkerne, geologische und geophysikalische Daten (inkl. 70 km^2 3D-Seismik) der Montanuniversität Leoben zur Verfügung gestellt. Ergebnisse verschiedener Studien, die auf diesen Daten beruhen, sind in diesem Artikel zusammengefasst.

Die Sedimentation im Trattnach-Feld startete im Jura mit klastischen Sedimenten und Plattformkarbonaten. Die Karbonate wurden in der Unterkreide gehoben und verkarstet. Fluviatile Sedimente (Schutzfels-Formation) füllten diese Karststrukturen auf. Flachmarine, ca. 30 m mächtige Sedimente aus dem Cenomanium (Regensburg- Formation) überlagern die Schutzfels-Formation oder jurassische Karbonate und weisen an der Basis häufig ein Transgressions-Konglomerat auf. Stark bioturbierte glaukonitreiche Sandsteine dominieren. Ein rötliches Konglomerat ("Marker Bed") und Kalksandsteine treten im oberen Teil auf. Tempestite und Schuttströme kommen häufig vor. Die cenomanen Sedimente werden von turonen kalkigen Tonen (Eibrunn- Formation) überlagert.

Die ältesten Strukturelemente stehen mit E-W-Kompression während Turonium/Coniacium in Verbindung, die auf die Öffnung des Nordatlantiks zurückzuführen ist. Die Bildung der Trattnach-Mega-Antiklinale und die transpressive Reaktivierung des NNW-

SSE-streichenden variszischen Schwanenstadt Störungssystems entstanden durch paleozäne NE-SW-gerichtete Kompression, die die Schließung des Penninischen Ozeans zur Folge hatte.

Eine Winkeldiskordanz charakterisiert die Grenze zwischen der mesozoischen Schichtfolge und eozänen klastischen und karbonatischen Gesteinen. Feinkörnige Gesteine des Unteroligozäns überlagern die Karbonate. Seismische Daten zeigen ausgedehnte submarine Rutschungen. Eine weitere Diskordanz trennt die Obere Puchkirchen-Formation (Egerium) von der Hall-Formation (Eggenburgium).

Als Folge der alpinen Gebirgsbildung und der Flexur des Südrandes der europäischen Platte bildeten sich im Känozoikum E-W-streichende Abschiebungen (Aistersheim- und Gaspoltshofen-Störungssysteme). Beide Störungssysteme wurden im frühesten Oligozän angelegt. Die Aktivität der Störungen nahm während des Egeriums ab und endete noch vor dem Eggenburgium. Die seismischen Daten belegen die Kippung des Blockes zwischen der Aistersheim- und der Gaspoltshofen-Störung während des späten Oligozäns.

Das Trattnach-Feld befindet sich innerhalb der Trattnach-Mega-Antiklinale. Die westliche Begrenzung wird vom Schwanenstadt-Störungssystem gebildet. Das Trattnach-Feld produziert Öl aus dem unteren Bereich der cenomanen Grünsandsteine (CE3, CE2). Die Reservoirqualität ist abhängig von der Korngröße, Tonmineralanteil und Karbonatzementation. Abgedichtet wird die Lagerstätte von cenomanen Gesteinen mit sehr geringer Permeabilitat (CE1) und von turonen kalkigen Tonen. Das Trattnach-Öl weist einen geringen Schwefelgehalt auf und ist gasuntersättigt. Die Ölakkumulation begann im Miozän. Das Wasser im Ölfeld weist eine niedrige Salinität auf. Das kann ein Hinweis auf eine hydraulische Verbindung mit meteorischen Wässern innerhalb der jurassischen Karbonatgesteine sein.

1. Introduction

The North Alpine Foreland Basin is a minor oil and moderate gas province (Fig. 1). After decades of exploration and with some 192 discoveries, the basin is considered mature in terms of hydrocarbon exploration (Veron, 2005). Many oil fields were detected in Eocene and Cenomanian reservoir horizons between the late 1950s and the 1970s. However, using advanced exploration tools and techniques, Rohöl-Aufsuchungs AG (RAG) recently has been successful in finding new fields and extending the life of old "brown" fields.

An example of a field, which produces oil since several decades, is the Trattnach Field situated at the northern slope of the North Alpine Foreland Basin in the central part of the Austrian sector (Fig. 1b). It was discovered in the year 1975 and produces oil from glauconitic sandstones with a Cenomanian age from a depth of approximately 1600 m. Surface elevation is about 500 m. With estimated oil in place of about 1.56 million tons, it is one of the medium sized oil fields in the Alpine Foreland Basin. The small Trattnach North Field was discovered about 2 km NNE of the main field in the same stratigraphic horizon in 1983.

Within the frame of a joint initiative between the Austrian oil industry (OMV, RAG) and Montanuniversitaet Leoben (PEPE; Petroleum Engineering Program of Excellence), RAG provided core material and a data set of the Trattnach Field including geological data, well logs from 16 wells and 3D seismic data covering an area of approximately 70 km^2 to Montanuniversitaet. Samples and data could be used for teaching purposes, diploma and doctoral thesis, as well as for project-based research work.

In the present contribution, we summarize the results of several studies related to the Trattnach area. These results are used to re-evaluate the evolution of the Trattnach area and to characterize the Trattnach Field.

2. Geological Setting

The North Alpine Foreland Basin (Molasse Basin) extends along the northern margin of the Alps from Geneva to Vienna (Fig. 1a). In the eastern sector, the northern margin of the basin is delineated by the outcropping basement of the Bohemian Massif. The southern part of North Alpine Foreland Basin is overthrust by Alpine nappes (Wagner, 1996).

2.1 Basin Fill

The crystalline basement with local NW- and NE-trending Permo-Carboniferous graben structures is covered by Mesozoic mixed carbonate-siliciclastic shelf sediments (Sissingh, 1997). The Mesozoic evolution commenced with deposition of Middle Jurassic fluvial sediments grading into marine sands. The clastic succession is overlain by Middle and Upper Jurassic carbonate rocks forming part of the South German carbonate platform (Brix and Schultz, 1993). Sponge banks, coral reefs and their debris occur within the carbonate platform. These rocks are overlain by salt lagoon and tidal flat deposits (Wagner, 1996). Carbonate deposition continued into earliest Cretaceous times (Wagner, 1996; 1998). Thereafter, the carbonate platform was uplifted and tilted, causing erosion and karstification.

The karst relief is filled locally by light-colored fluvial sandstones with sporadic clay layers (Schutzfels Formation; Fig. 5). Niebuhr et al. (2009) assume an Early Cretaceous age for the Schutzfels Formation. Pantic (in Nachtmann, 1995) detected pollen and spores characteristic for the Albian/Cenomanian boundary. Thereafter, a major Cenomanian transgression from SW led to the deposition of storm influenced marine sediments on the northern shelf of the Helvetic Sea (Nachtmann and Wagner, 1987). They consist mainly of glauconitic fine to coarse grained sandstones. Because of the similarities to green sandstones in the Regensburg area (Trusheim, 1935), Wagner (1998) attributed these sandstones to the Regensburg Formation (Fig. 2), which has been subdivided into a lower Saal Member and an upper Bad Abbach Member by Niebuhr et al. (2009).

On-going subsidence during Turonian time resulted in deposition of dark deeper-water marls (Eibrunn Formation; Niebuhr et al., 2009). The Eibrunn Formation is overlain by Turonian-age glauconitic sandstones and marls and sandstones of Coniacian to Late Campanian age. Uplift of the European plate at the end of the Cretaceous led to erosion of significant parts of Mesozoic sediments.

The Molasse stage of basin evolution developed since Late Eocene times in response to loading of the southern margin of the European plate after the Alpine orogeny (Bachmann et al., 1987; Genser et al., 2007). The Eocene sedimentary succession is characterized by floodplain deposits, meandering channels and limnic deposits of the Voitsdorf Formation overlain by brackish-water Cerithian Beds and shallow marine Lithothamnium Limestone (Wagner, 1998; Rasser and Piller, 2004).

During Early Oligocene time, the North Alpine Foreland Basin deepened and widened abruptly (Sissingh, 1997) resulting in the deposition of deeper-water sediments (Schöneck, Dynow, Eggerding and Zupfing formations; Fig. 2). Submarine mass movements occurred during deposition of the Eggerding Formation (Sachsenhofer and Schulz, 2006; Sachsenhofer et al., 2010). During Late Oligocene to Early Miocene times dee-

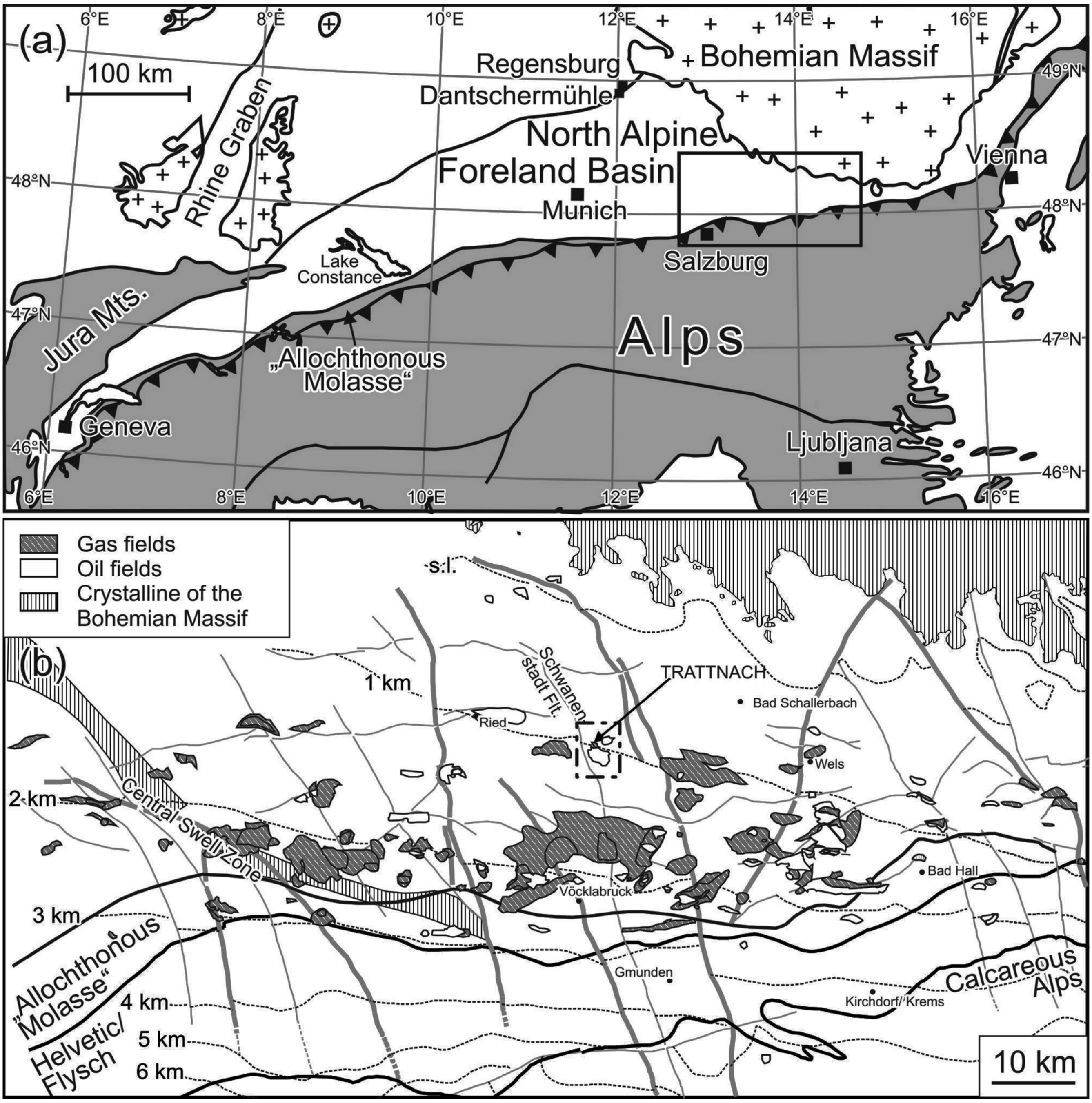

Figure 1: a) Sketch map of the Molasse Basin extending from Geneva to Vienna. The black rectangle marks the area of Fig. 1b. b) Location of oil and gas fields in the Austrian part of the Molasse Basin. The rectangle shows the position of the Trattnach 3D cube. The fault pattern and depth of base Eocene (in km below mean sea level) are shown after Wagner (1998) and Kröll et al. (2005).

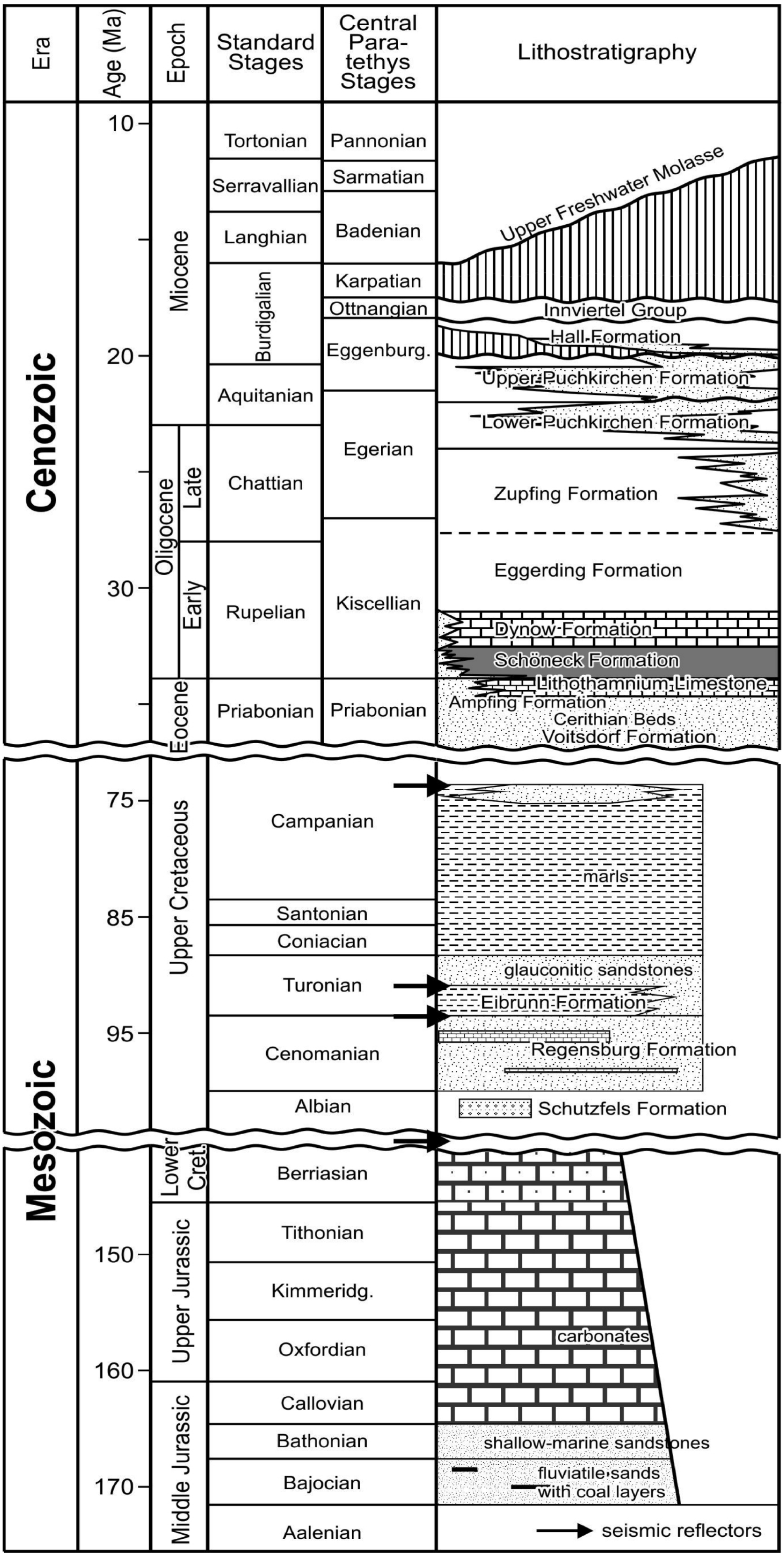

Figure 2: Stratigraphy of the fill of the Alpine Foreland Basin (modified after Malzer et al., 1993; Wagner, 1998; Grunert et al., 2015).

per marine conditions persisted E of Munich (Puchkirchen Basin), whereas a deltaic complex filled the western part of the North Alpine Foreland Basin (De Ruig, 2003). Shallow marine sandstones were deposited along the northern basin margin. The deeper-marine Puchkirchen Group is characterized by a thick succession of gravity-flow deposits consisting of gravel, sandstones and shales. These deposits are encased by deeper-marine shales. The Puchkirchen Group is separated from the deeper-marine lower part of the Early Miocene Hall Formation by a major subaqueous erosional hiatus (Base Hall Unconformity).

The Hall Formation is characterized by a thick succession of shales with thin turbidites and tempestites in the lower part (Borowski, 2007). The upper part of the Hall Formation is characterized by the progradation of deltas from the S (Grunert et al., 2013). The basin was finally filled with sediments of the Innviertel Group. At the end of the Lower Miocene the Austrian part of the North Alpine Foreland Basin was tilted towards the west (Gusterhuber et al., 2012). Coal-bearing limnic and fluvial sediments of Middle and Late Miocene age (Freshwater Molasse) follow above the erosional unconformity. The entire area was uplifted after deposition of the Freshwater Molasse and sediments 500 to 900 m thick have been eroded (Gusterhuber et al., 2012).

2.2 Petroleum Systems

Two distinct petroleum systems occur in the Austrian part of the North Alpine Foreland Basin: a Mesozoic to lower Oligocene oil and thermal gas system and an Oligo-/Miocene microbial gas system (Wagner, 1998).

Lower Oligocene deeper-water sediments are the source rocks for oil and minor thermal gas (Sachsenhofer et al., 2010). The Schöneck Formation with organic carbon contents up to 12 % and mean Hydrogen Index values between 500 and 600 mgHC/gTOC is the most prolific source rock interval (Schulz et al., 2002). The source rocks are immature in areas of the oil fields and enter the oil window (4–6 km depth) only beneath the Alpine nappes indicating long-distance migration (Schmidt and Erdogan, 1996; Gratzer et al., 2011; Bechtel et al., 2013). Hydrocarbon generation started during Miocene thrusting (Gusterhuber et al., 2013; 2014). Most important oil reservoirs are located in Upper Eocene basal sandstones, typically on the upthrown side of E-W trending S- and N-dipping normal faults. Some oil is trapped in Mesozoic (e.g. Cenomanian sandstones) and Oligocene horizons as well as in Eocene carbonates. Gratzer et al. (2011) distinguished an eastern and a western oil family and related them to differences in the facies of the Lower Oligocene source rocks.

Reservoirs for microbial gas are Late Oligocene (Lower Egerian) and Miocene (Upper Egerian, Eggenburgian) turbiditic sandstones and sandy conglomerates. Stratigraphic and compaction structures, or a combination of both, and imbrication structures form major traps for the microbial gas. Although thermal and microbial hydrocarbons are typically separated by fine-grained sediments, several hundred metres thick, compositional and isotopic data suggest mixing of thermal and microbial gases (Reischenbacher and Sachsenhofer, 2011).

3. Database and Methods

3.1 Database

The study of the Trattnach area is based on a 3D seismic cube covering an area of approximately 70 km^2 and data from 16 wells. Most of the wells terminate near the base of the Cenomanian and only a few wells drilled into the Jurassic carbonate platform. A full set of geophysical logs was available for the present study. However, logs of formations overlying the Hall Formation are often missing. Gamma ray (GR), sonic (DT) and resistivity logs are shown in the present paper. Checkshots were available for 10 wells. Further geological control was provided by sedimentological and spectral core gamma ray logs of borehole cores recovering the Regensburg Formation, and porosity/permeability data.

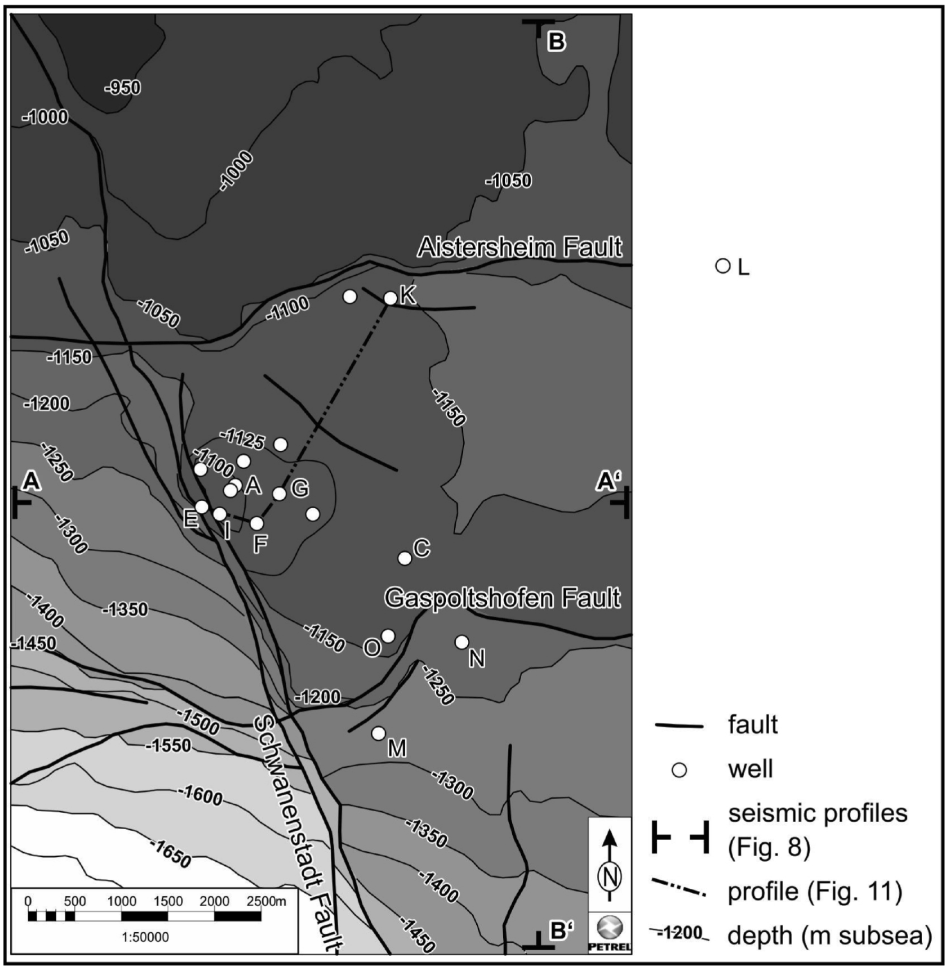

Figure 3: Structure map of Top Cenomanian. The location of key wells and the position of an inline and a crossline (Fig. 8) and of a correlation panel (Fig. 11) are shown.

3.2 Interpretation of stratigraphic horizons and faults

Key horizons were identified by matching synthetic seismograms and 3D seismic data. Horizons were mapped using Petrel® Software on variable inline and crossline spacing (bin size is 25*25 m) depending on resolution and traceability of the reflector. The horizons identified are: Top Crystalline Basement (Top XBM), Top Jurassic (= Base Cenomanian), Top Cenomanian, Top Turonian marl (Top TRTNM), Base Eocene (=Top Mesozoic), Base Puchkirchen Formation (Base PS), Top Lower Puchkirchen Formation (Top LPS; = Base Upper Puchkirchen Fm.), Base Hall Formation. In addition, some intra-formational horizons were mapped.

Isochrons were generated for each of the stratigraphic intervals defined by these horizons. Furthermore, seismic attributes were calculated and analyzed, including horizon attributes, 3D attributes and horizon slices, to aid in the interpretation of detailed subsurface geometries and tectonic fractures at a field scale. The "Ant-track" 3D seismic attribute generated in Petrel® software was used for determination of faults (Pederson et al., 2002; Cox and Seitz, 2007).

3.3 Analytical Work

Sedimentological logging of cores of the Regensburg Formation is obtained from wells of the Trattnach area. Conventional sediment petrographic methods (e.g. microscopy, X-ray diffractometry, cathodoluminiscense, SEM) were applied to establish the mineralogy and diagenetic history of the siliciclastics. Bulk geochemical data (carbon, sulphur, RockEval pyrolysis) from fine-grained rocks were measured according to established procedures (see Sachsenhofer et al., 2010).

4. Geological Setting and evolution of the Trattnach area

4.1 Sedimentary record and log facies

4.1.1 Mesozoic succession

Pre-Eocene erosion removed large parts of the Cretaceous succession in the Trattnach Field. Therefore, well L, located 1 km east of the 3D cube has been selected for the discussion of log patterns (Fig. 4).

Jurassic: Jurassic rocks overlie gneiss of the Bohemian Massif (well A). The lower part of the Jurassic succession, 22 m thick, is characterized by fluvial to shallow marine clastic rocks with strongly varying GR values. The overlying extensive carbonate platform with (oolithic) limestone and dolostone is characterized by very low GR and DT readings. In well L the carbonate platform is only 52 m thick, but reaches 135 m in the Trattnach Field. The surface of the Malmian carbonate platform is strongly karstified and locally filled by Schutzfels Formation.

Lower Cretaceous (?; Schutzfels Fm.): Schutzfels Formation is missing in well L, but 12 m of this formation have been cored in well E. Here, it is composed of white fluvial sandstone, often quartz rich and cemented by kaolinite. 2-m-thick dark-coloured floodplain deposits occur in the lower part. Fossil char coal is the dominant organic matter. Paleosoil was drilled beneath a Cenomanian transgressive conglomerate (Fig. 5).

Cenomanian (Regensburg Fm.): Cenomanian rocks overlie the Schutzfels Formation or rest directly on the karstified Jurassic carbonate platform. The Malmian surface often shows piddock holes. A transgressive conglomerate with carbonate clasts is developed at the base of the Regensburg Formation (well E; Fig. 6a,d).

A detailed description of the 30-m-thick Cenomanian succession follows in section 5 describing the Trattnach Field. Here the log response of the green sandstones and possible pitfalls are described briefly. We used the following methods: gamma ray log (GR), acoustic (sonic) log (DT), resistivity (MLL).

The GR log shows a high vertical variability. GR logs in green sands are often strongly influenced by K-bearing glauconite. However, spectral core gamma ray data from borehole F show that in the case of the Cenomanian in the Trattnach area, the GR log is mainly controlled by thorium present in heavy minerals (e.g. monazite) and not by potassium in glauconite (Fig. 7). In any case, the GR log is not a good tool to distinguish shale and sand in the Regensburg Formation. DT and resistivity (MLL) logs reflect the degree of carbonate cementation. The lower part (CE3 acc. Nachtmann, 1995) is characterized by upward increasing DT values, the middle part displays high DT values, whereas the upper part (CE1) is characterized by relatively low DT readings and high resistivity values due to high carbonate contents.

Turonian-Coniacian: GR and DT logs reflect the transgressive trend of the Turonian succession. A maximum flooding surface

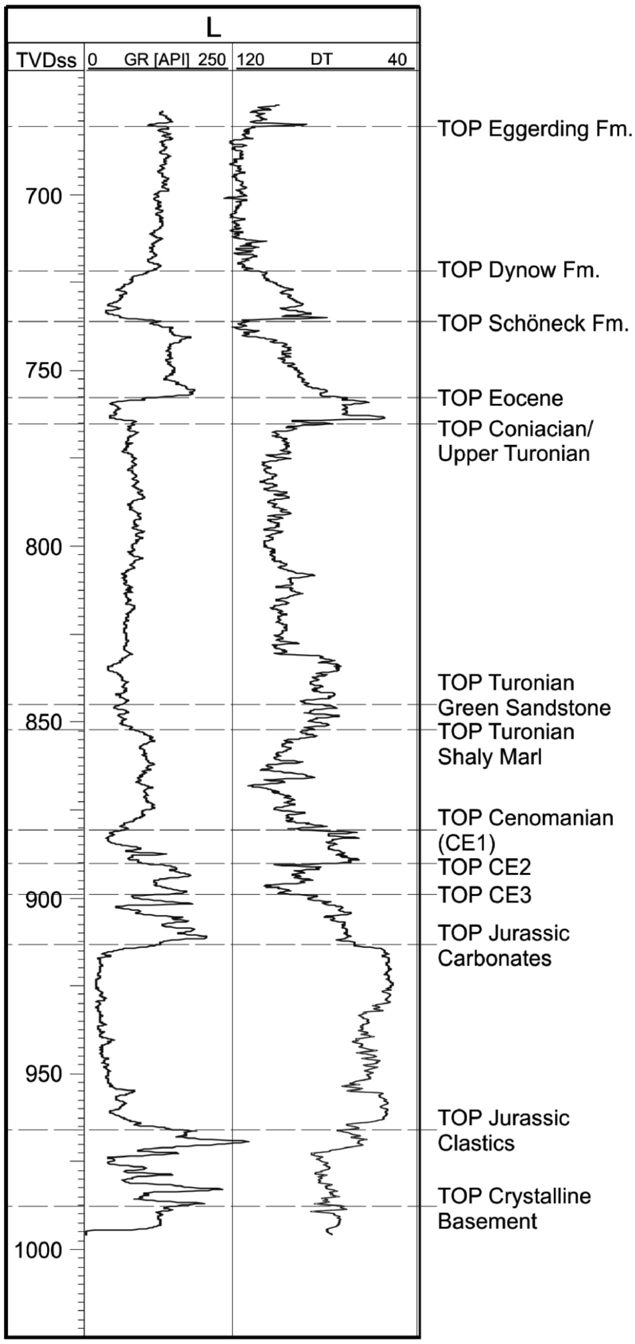

Figure 4: Gamma ray (GR) and sonic log (DT) of the Mesozoic to Lower Oligocene section in well L.

(mfs) located about 12 m above the Cenomanian sandstones within the Turonian shaly marls (Eibrunn Fm.) separates the transgressive from a regressive, coarsening-upward trend (upper part of Eibrunn Fm., Turonian glauconite sandstone, lowermost Coniacian). In well L the upper boundary of the coarsening upward trend, 37 m thick, is sharp (Fig. 4). In many other wells it is gradual.

According to Wilmsen et al. (2010) stable isotope data show that the lower part of the Eibrunn Formation in the Regensburg area has been deposited during the Cretaceous Anoxic Event OAE2 (Schlanger et al., 1987). In order to test whether the OAE2 can be found in Upper Austria and to explore whether it has any effect on the source rock potential, bulk geochemical parameters of the lower 16 m of the Eibrunn Formation in the Trattnach Field have been determined. Carbonate contents within this interval range from 3 to 36 % and classify the rocks as calcareous shale. TOC contents vary between 0.3 and 1.4 % respectively. Whereas TOC contents might indicate some fair hydrocarbon potential, HI values constantly below 22 mgHC/gTOC show that the investigated succession does not hold any significant hydrocarbon potential (Peters, 1986). The organic matter is immature (Tmax: 422-428°C; vitrinite reflectance of Cenomanian in well G: 0.49+/-0.06 %Rr).

The upper part of the Coniacian, 67 m thick, is characterized by a uniform marl succession. The top of the Coniacian is formed by an erosional unconformity.

4.1.2 Cenozoic succession

The Eocene succession in the Trattnach area is only a few meters thick. In well L the lower sandstone unit is 2.6 m thick, whereas carbonate rocks (Lithothamnium Limestone) reach a thickness of 5.2 m. The Eocene succession shows a blocky GR pattern. Low DT readings coincide with the limestones.

Generally high, but varying GR and DT readings reflect different carbonate contents of the organic-rich, fine-grained Schöneck Formation, which has been studied in some detail in well L. The lowermost 2.5 m of this formation are silty, bioturbated and contain only 0.5 % TOC. A marl interval (units "a, b" according to Schulz et al., 2002) contains 2.1 % TOC in average with an HI of about 400 mgHC/gTOC, classifying the organic matter as kerogen type IIb. The uppermost shale unit "c" contains strongly varying TOC contents (2.5 – 9.5 %) and HI values ranging from 400 to 600 mgHC/gTOC (kerogen Typ IIa). Similar to the Turonian, the Schöneck Formation is immature (Tmax: ~420°C).

The Schöneck Formation is overlain by limestones and marls of the Dynow Formation. Upward increasing GR and DT readings reflect upward decreasing carbonate contents (Schulz

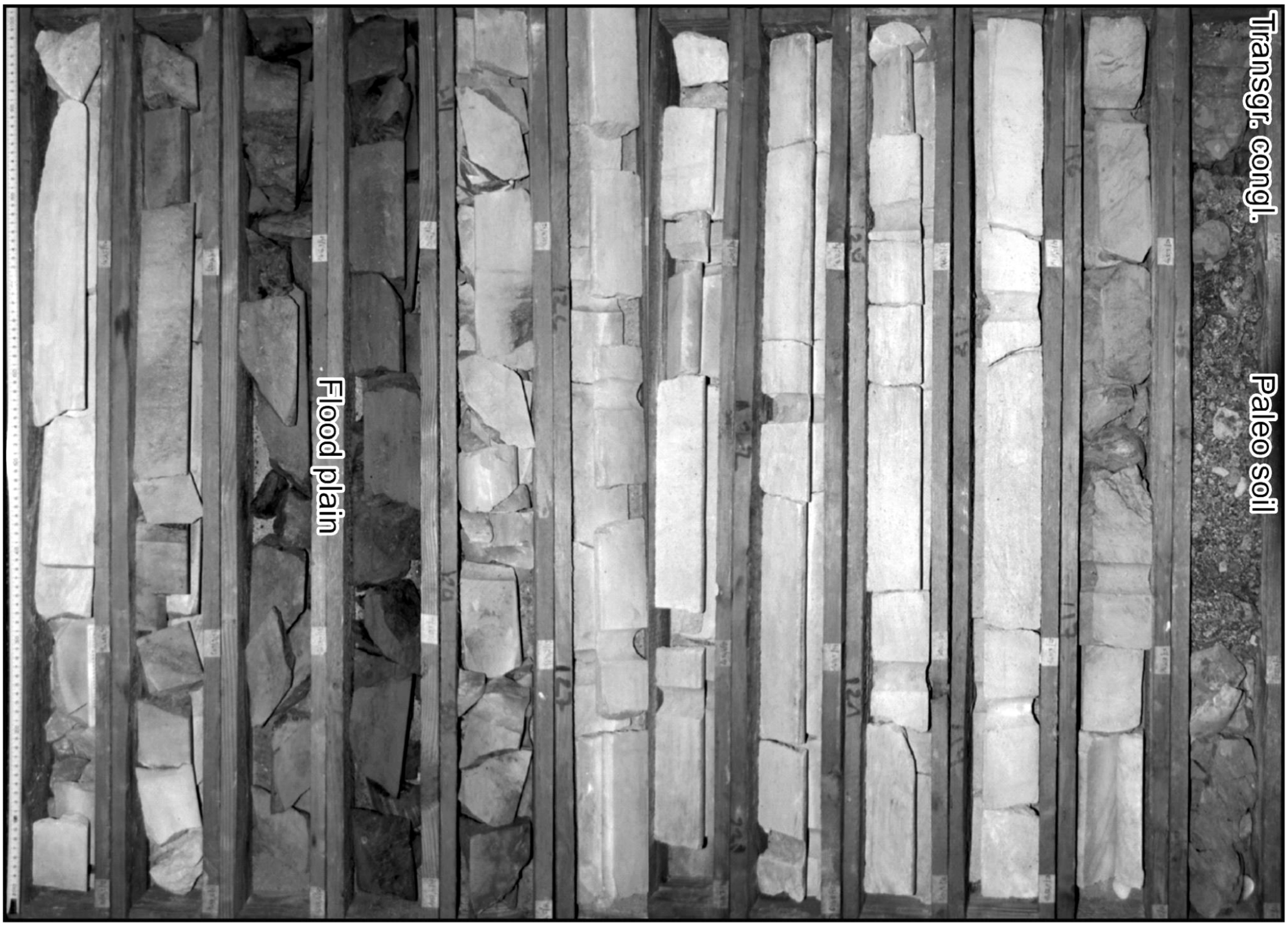

Figure 5: Schutzfels Formation in well E.

et al., 2005) The Dynow Formation passes upwards into shales with low carbonate contents (Eggerding Fm.) which are overlain by calcareous shales of the Zupfing Formation. Because of the different carbonate content the boundary between the Eggerding and Zupfing formations is characterized by a decrease in GR and DT (Sachsenhofer et al., 2010).

Whereas, a complete Lower Oligocene succession is present in well L, Lower Oligocene layers are partly missing in the well F (Sachsenhofer and Schulz, 2006).

4.2 Seismic characterization of the stratigraphic record

One inline (N-S trending) and one crossline (E-W trending) of the 3D seismic data are shown in Fig. 8 to illustrate the seismic characteristics of the main stratigraphic units.

4.2.1 Mesozoic succession

The base of the Mesozoic succession is formed by Top Crystalline Basement (Top XBM). Its definition is based on well tops of wells A, M, N, and O and a tentative mapping of a discontinuous, low amplitude reflector (negative amplitude) associated with these well tops. Note that the reflector cannot be traced with adequate reliability.

Jurassic: The Top Jurassic (= Base Cenomanian/Cretaceous) was defined as a reflector with strong negative amplitude (Fig. 8). It is easily traceable across the whole study area. An angular unconformity between Jurassic and Cretaceous deposits, known from other parts of the North Alpine Foreland Basin (Nachtmann and Wagner, 1987), is not developed in the study area.

The TWT-thickness map of the Jurassic succession shows a general increase in thickness from NE to SW from 40 to 80 ms (Fig. 9e). An area with higher thickness near the eastern margin of the study area may be due to difficulties related to the mapping of Top XBM. The Jurassic succession is 120-140 m thick in wells A and O.

The basal clastic and the overlying carbonate rocks cannot be distinguished clearly in the seismic data. Intra-Jurassic reflectors are typically of low frequency and often blurred. Their lateral continuity decreases towards the north. The varying seismic facies reflects lithology variations within the carbonate platform (see also von Hartmann et al., 2012).

The amplitude of the Top Jurassic (Base Cenomanian) reflector decreases in NE direction. Evidence for karstification of the

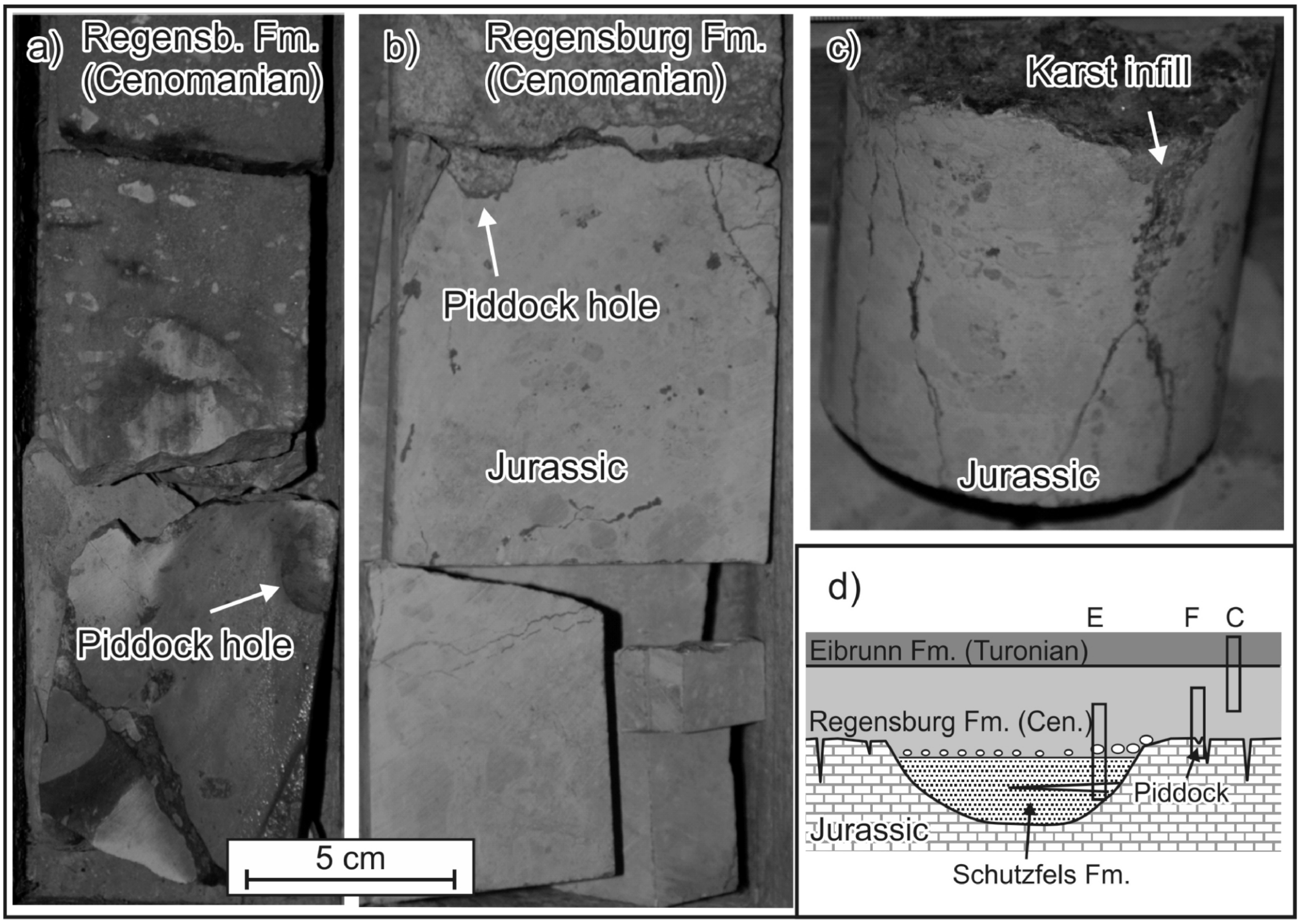

Figure 6: a) Transgressive conglomerate at the base of the Regensburg Formation (well E). Note piddock hole in one of the carbonate clasts. b) Piddock hole in Jurassic limestone underlying Regensburg Formation (well F). c) Karst infill in Jurassic limestone breccia (well F). d) Cartoon showing the karstified surface of the Jurassic carbonate platform and its relation to Schutzfels, Regensburg and Eibrunn formations (simplified after Oschmann, 1958). Rectangles indicate position of cored intervals in wells E, F, C.

Jurassic carbonates cannot be observed. However, karstification and infill of these karst structures by the Schutzfels Formation is well documented in the study area (see below).

Cretaceous: The Top Cretaceous (= Base Eocene) is a major angular unconformity truncating intra-Cretaceous reflectors. It is formed by a continuous high amplitude reflector. The thickness distribution of the Cretaceous succession (Fig. 9d) is controlled by pre-Eocene deformation and erosion. Areas with low thickness (40 ms; ~60 m) reflect a large-scale anticlinal dome, which is truncated by the pre-Eocene unconformity. The preserved thickness of the Cretaceous succession in the downthrown block west of the NNW trending Schwanenstadt Fault is significantly higher (up to 210 ms) because of lesser erosion (Fig. 9e).

Two additional stratigraphic horizons were mapped within the lower part of the Cretaceous succession, the Top Cenomanian and the Top Turonian Shaly Marl.

- Top Cenomanian (Top Regensburg Fm.) is defined as a reflector with negative amplitude (Fig. 8). The reflector is well traceable and continuous throughout the entire seismic cube. The TWT-thickness of the Cenomanian succession is in the range of 10 to 20 ms (15 - 35 m). There is no obvious lateral thickness trend. The seismic facies is laterally uniform with parallel, continuous, high amplitude reflectors defining Base and Top Cenomanian and one internal reflector.
- The Top Turonian Shaly Marl (Top TRTNM; Eibrunn Fm. of Niebuhr et al., 2009) forms an excellent traceable high amplitude reflector (Fig. 8). It roughly corresponds to the Turonian mfs. Progradations of glauconitic sandstones of Turonian age above the mfs are indicated by well logs, but are not resolved in seismic data.

Pre-Eocene erosion removed large parts of the Coniacian to Maastrichtian(?) succession and locally even cut into the Turonian (e.g. well I). Therefore, the seismic facies of Coniacian to Campanian(?) sediments can be studied only west of the Schwanenstadt Fault where the sediments are characterized by parallel, continuous, low amplitude, medium frequency reflectors.

4.2.2 Cenozoic succession

The following main reflectors have been mapped in the entire study area (from base to top): Base Puchkirchen Formation (= Top Zupfing Fm.), Top Puchkirchen Formation (= Base Hall Fm.).

Eocene and Lower Oligocene (Schöneck – Zupfing Fm.): The reflector defining the top of the Lower Oligocene is well constrained by well tops and synthetic seismograms. It is characterized by a continuous, low amplitude reflector.

Reflection configuration along the N-S section shown in Fig. 8 indicates the presence of a submarine erosion (reflector c in Fig. 8a), which removed Dynow Formation, Schöneck Formation and parts of the Eocene in the southern part of the study area (Sachsenhofer et al., 2010). Internal reflectors are continuous and parallel. In undisturbed areas (e.g. northern part of line shown in Fig. 8a) a tripartition is indicated by differences in amplitude: Eocene, Schöneck and Dynow formations are characterized by high amplitude reflectors, Eggerding Formation by reflectors with moderate amplitude and the Zupfing Formation by low-amplitude reflectors.

The isochron map of the interval between Base Eocene and Top Eggerding Fm (Fig 9c) shows that the entire Lower Oligocene succession is preserved only in the NE part of the study area. In the remaining part, the Lower Oligocene succession is missing due to large submarine mass movements (Linzer and Sachsenhofer, 2010; Sachsenhofer et al., 2010). Nowadays this material is located beneath the Alpine nappes. However, parts of the sliding material remained in the Trattnach area forming the mega-slide indicated in Fig. 9c. Its extension suggests that the Aistersheim fault system was not active during sliding. Slide scarps bounding the main mass movement are W-E and N-S trending.

The TWT-thickness of the sedimentary package between Base Eocene and Base Puchkirchen Formation ranges between 100 and 160 ms (~140 to 200 m) and increases in north(east)ern directions (Fig. 9b). The considered area is too small to derive regional thickness trends. However, it is worth mentioning that the same thickness variation (maxima parallel to the WNW trending paleo-shore line) has been observed in the shaly part of Schöneck Formation and in the Dynow Formation (Sachsenhofer and Schulz, 2006).

Upper Oligocene – Early Miocene (Lower and Upper Puchkirchen Fm.): Top Puchkirchen Formation (Base Hall Fm.) is repre-

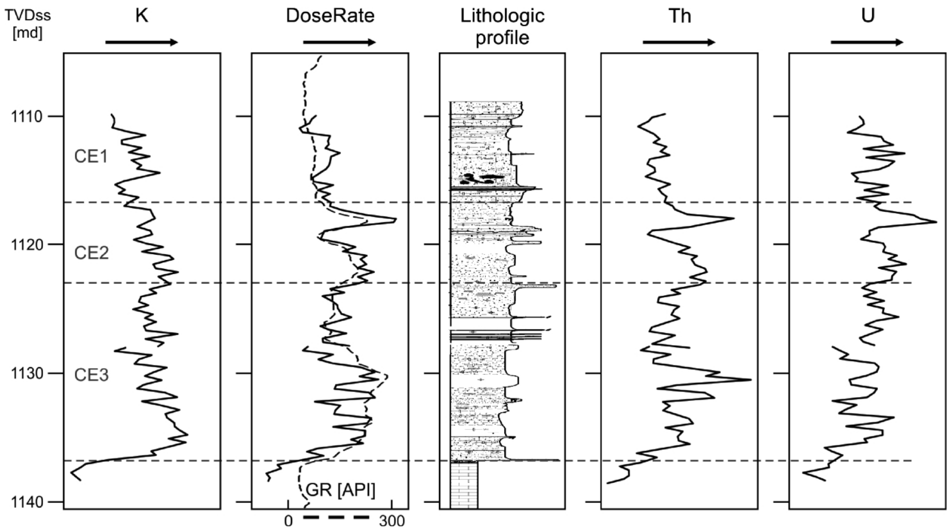

Figure 7: Lithologic profile, GR log and K, Th, U, and Dose Rate from spectral core gamma measurments of well F.

sented by a southward dipping reflector truncating the upper part of the Puchkirchen Formation. Reflectors above Top Puchkirchen Formation terminate in an onlap relation. The position of the reflector is supported by good well control.

The TWT-thickness map of Puchkirchen Formation shows values between 250 and 400 ms with relatively low thicknesses north of the Aistersheim and Gaspoltshofen faults systems (Fig. 9a). Thickness variations are caused by an interplay of

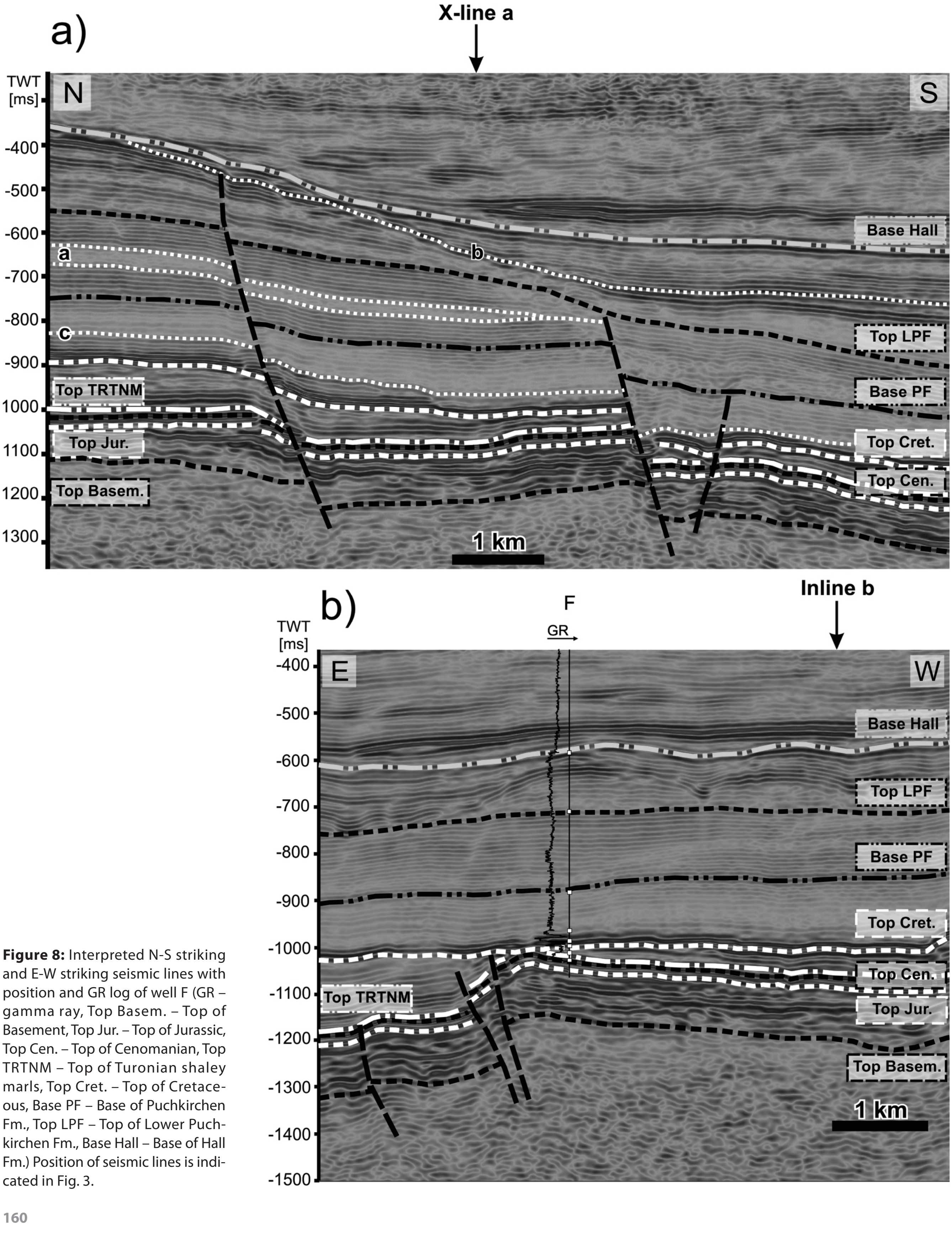

Figure 8: Interpreted N-S striking and E-W striking seismic lines with position and GR log of well F (GR – gamma ray, Top Basem. – Top of Basement, Top Jur. – Top of Jurassic, Top Cen. – Top of Cenomanian, Top TRTNM – Top of Turonian shaley marls, Top Cret. – Top of Cretaceous, Base PF – Base of Puchkirchen Fm., Top LPF – Top of Lower Puchkirchen Fm., Base Hall – Base of Hall Fm.) Position of seismic lines is indicated in Fig. 3.

syn-tectonic deposition and deep (Base Hall) erosion. N-S trending canyons are visible in the northern part of Fig.9a. Their orientation is roughly perpendicular to the deep-marine channel belt filling the Puchkirchen Basin south of the Trattnach area (De Ruig, 2003; De Ruig and Hubbard, 2006).

The Lower Puchkirchen Formation is separated from the Upper Puchkirchen Formation by a continuous reflector. The seismic facies suggests a tripartition of the Lower Puchkirchen Formation. A lower part is characterized by parallel reflectors with moderate amplitudes, which are blurry near the Gaspoltshofen Fault System. North of these faults, this facies is conformably overlain by a northward thickening, wedge-shaped unit with low amplitude reflectors (a in Fig. 8a). A succession of parallel medium-amplitude reflectors forms the uppermost part of the Lower Puchkirchen Formation.

The Upper Puchkirchen Formation is subdivided by a south-

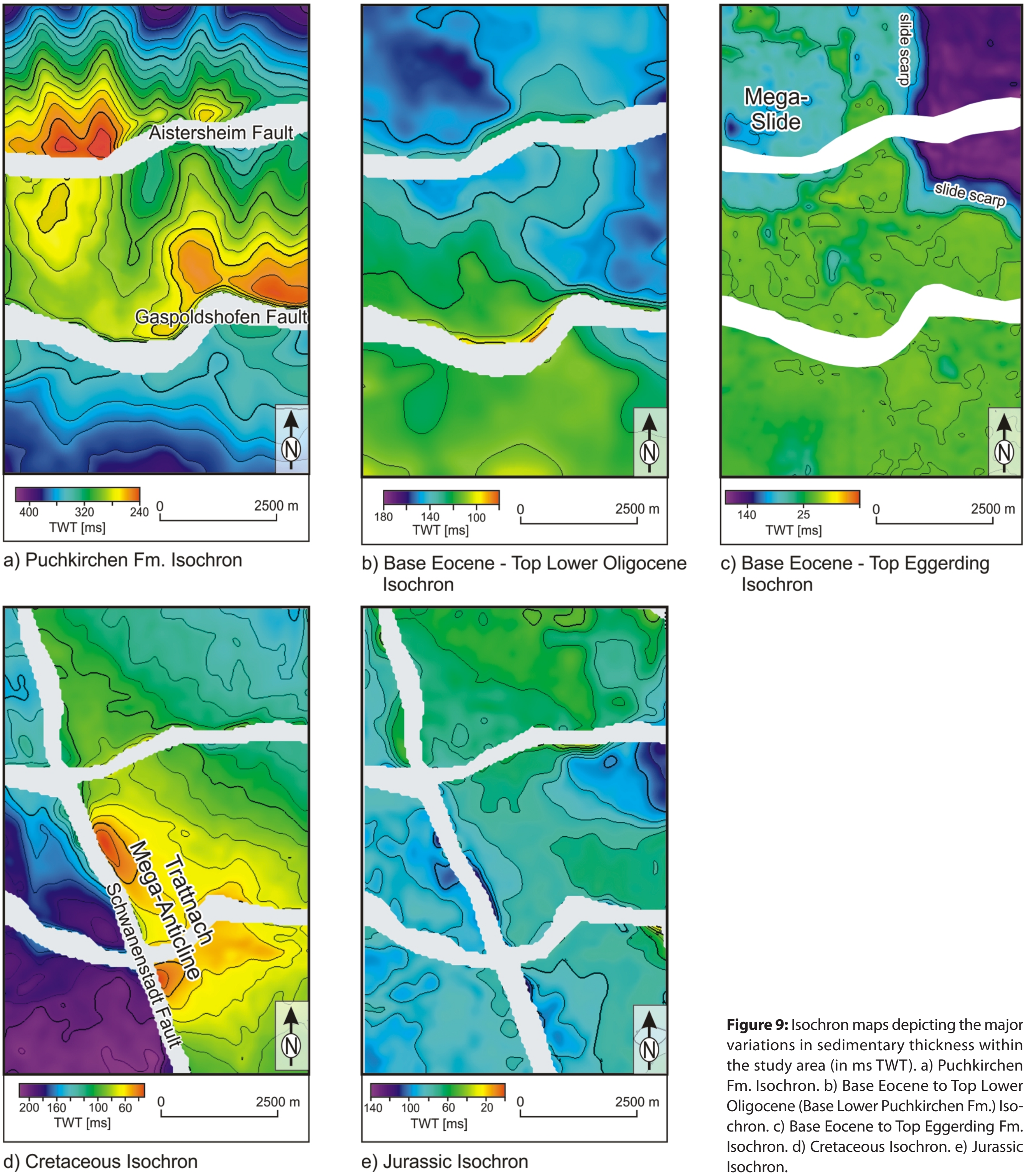

Figure 9: Isochron maps depicting the major variations in sedimentary thickness within the study area (in ms TWT). a) Puchkirchen Fm. Isochron. b) Base Eocene to Top Lower Oligocene (Base Lower Puchkirchen Fm.) Isochron. c) Base Eocene to Top Eggerding Fm. Isochron. d) Cretaceous Isochron. e) Jurassic Isochron.

ward dipping erosional surface (reflector b in Fig. 8a), which is more prominent than the Base Hall erosion surface in the study area. Sediments overlying the intra-Puchkirchen erosional surface show an onlap relation.

4.3 Deformation structures and structural evolution

4.3.1 Turonian/Coniacian structures

The oldest tectonic structure visible in the study area is a N-S trending bulge, about 3 km long, in the western part of the study area (T1 in Fig. 10a). Its steep western flank is confined by an E-dipping fault with a reverse component (Figs. 8b, 10b). Top TRTNM is the uppermost deformed reflector arguing for a Late Turonian to Early Coniacian deformation phase. Similar structures are visible near the northeastern margin of the study area and may be related to Middle to Late Turonian inversion tectonics at the southwestern margin of the Bohemian Massif (Niebuhr et al., 2011, 2014).

Based on the orientation of the N-S trending structures a W-E horizontal stress regime is suggested (e.g. Butler, 1982). W-E compression may be related to the coeval opening of the N-Atlantic (Ziegler, 1987), which affected the study area situated at the southern shelf of the European continent.

4.3.2 Maastrichtian?/Paleocene structures

The dominant pre-Eocene structural element, however, is a NNW-SSE-trending fault system (Schwanenstadt Fault sensu Wagner, 1998). This fault system separates a western part with thick Cretaceous sediments from the eastern part, where Cretaceous rocks are relatively thin due to significant erosion. The vertical throw of the Schwanenstadt Fault increases from north to south from 40 to 100 ms TWT (~50 to 200 m). Its steep dip suggests strike-slip movements with a reverse fault component. In analogy to similar faults in the foreland basin and in the Bohemian Massif it may by assumed that the Schwanenstadt fault system started as a dextral strike-slip fault during late Variscan time and was reactivated in the Early Jurassic, Early Cretaceous and early Paleogene (Brandmayr et al., 1995; Wagner, 1998). Associated reverse and normal faults (e.g. a, b in Fig. 10a) occur east of the Schwanenstadt fault system. Some of these faults have been reactivated during Cenozoic time as normal faults.

Erosion of Cretaceous rocks reached a maximum east of the Schwanenstadt Fault forming a large anticlinal dome (Trattnach Mega-Anticline; Fig. 9d). The Trattnach Mega-Anticline exhibits two culminations. The northern one hosts the Trattnach Field (Fig. 9d). Deep truncations and angular unconformities reflect intense erosion during Late Cretaceous and Early Cenozoic times. Erosion in the area of the Trattnach Mega-Anticline cut into Turonian horizons. In contrast Coniacian, Santonian and possibly even younger Cretaceous rocks are preserved in the western study area.

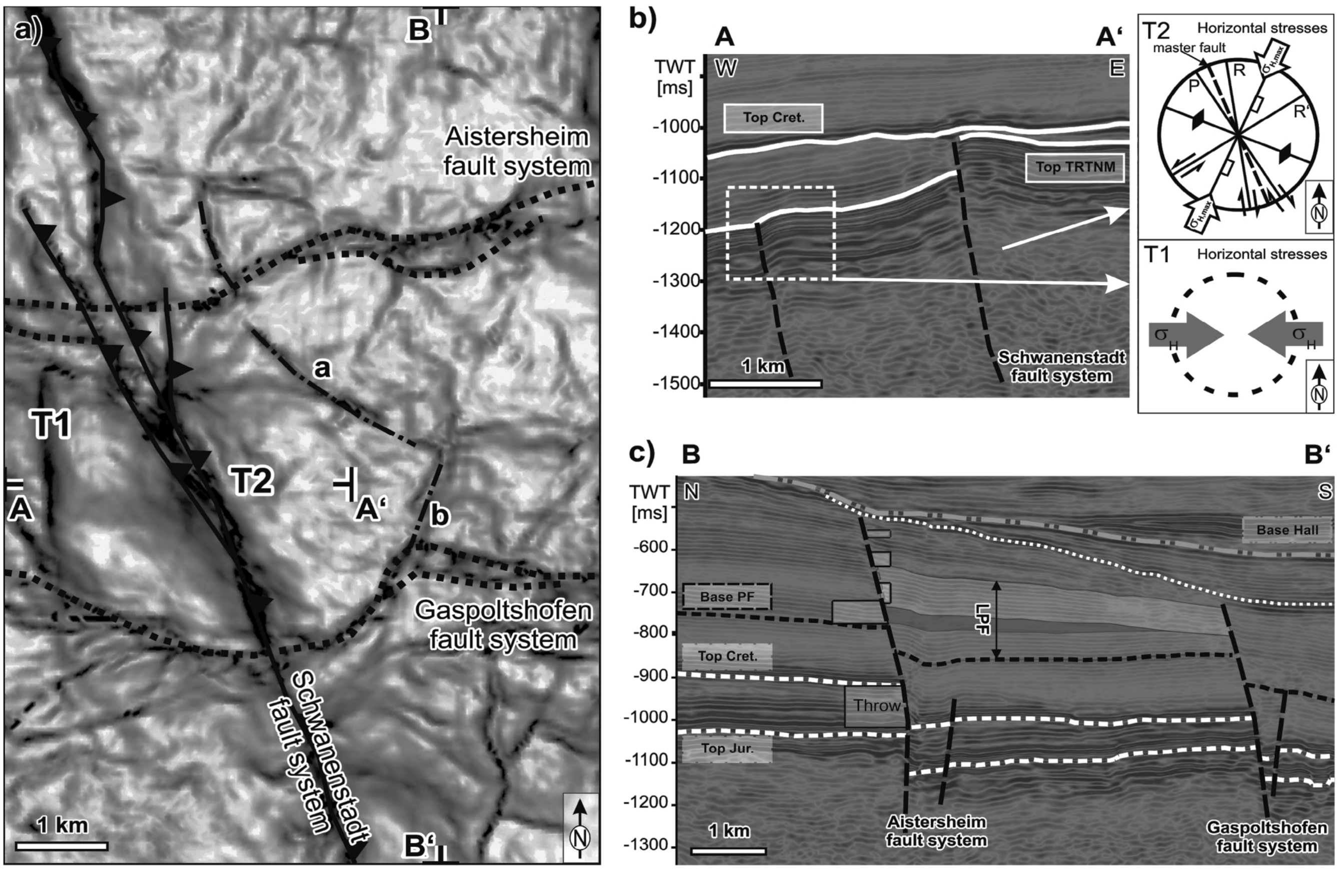

Figure 10: a) Relief map of Top Cenomanian. A-A' and B-B' represent profiles shown in b) and c). b) Mesozoic faults and associated horizontal stresses. c) Cenozoic faults. Note that throws increases downwards (LPK = Lower Puchkirchen Fm.).

Paleocene deformation events, including formation of the Trattnach Mega-Anticline, result from intraplate compressional stresses related to the closure of the Penninic Ocean (Dèzes et al., 2004). Intraplate forces were NE directed towards the Bohemian Massif, which was acting as a rigid block. Compression caused dextral reactivation of the Schwanenstadt Fault in a transpressional regime. In addition, some smaller NW-SE trending faults, including fault "a" E of the Trattnach Anticline, can also be linked to this event (Fig. 10a).

NNE-SSW transpression caused a dextral master fault with R, P and R' faults (Fig. 10b). In addition a reverse fault (NW-SE trending), and a normal fault (NE-SW trending; b in Fig. 10a) occur within the study area.

4.3.3 Post-Eocene (Oligocene-Early Miocene) structures

Formation of E-W trending normal faults and reactivation of older fault systems are the main deformation events affecting Cenozoic successions. Normal faulting is related to flexural down-bending due to the approaching Alpine thrust sheets during latest Eocene and Oligocene time.

Two major normal fault zones are present in the study area (Aistersheim fault system in the N, Gaspoltshofen fault system in the S; Figs. 3, 10). Both systems show a main S-dipping fault plane and a generally subordinate N-dipping (antithetic) fault plane and were activated during earliest Oligocene (Figs. 8, 10c) time. Fault segments with orientations which do not fit to the predominantly E-W trending direction (e.g. SW-NE trending segment of the Gaspoltshofen Fault) reflect reactivations of older faults. The activity of the Cenozoic deformation phase decreased during deposition of the Lower Puchkirchen Formation (early Egerian) and stopped after deposition of the Upper Puchkirchen Formation (end of the Egerian; earliest Miocene; Figs. 8, 10c).

Tilting of the fault block confined by the Aistersheim and Gaspoltshofen faults (Trattnach Block) during Late Oligocene (early Egerian) time is reflected by the northward thickening of unit "a" within the Lower Puchkirchen Formation (Fig. 8a; grey shaded layer in Fig. 10c). Whereas unit "a" changes its thickness laterally in the Trattnach Block, its thickness is uniform in the block north of the Aistersheim fault system. Cenozoic block tilting has not yet been described in the Austrian part of the North Alpine Foreland Basin. Theory and constraints of block rotation in collisional foredeeps are described by Bradley and Kidd (1991). They conclude that rotational backtilting of fault blocks is a common feature associated with flexural extension and down-bending of the lithosphere in collisional processes.

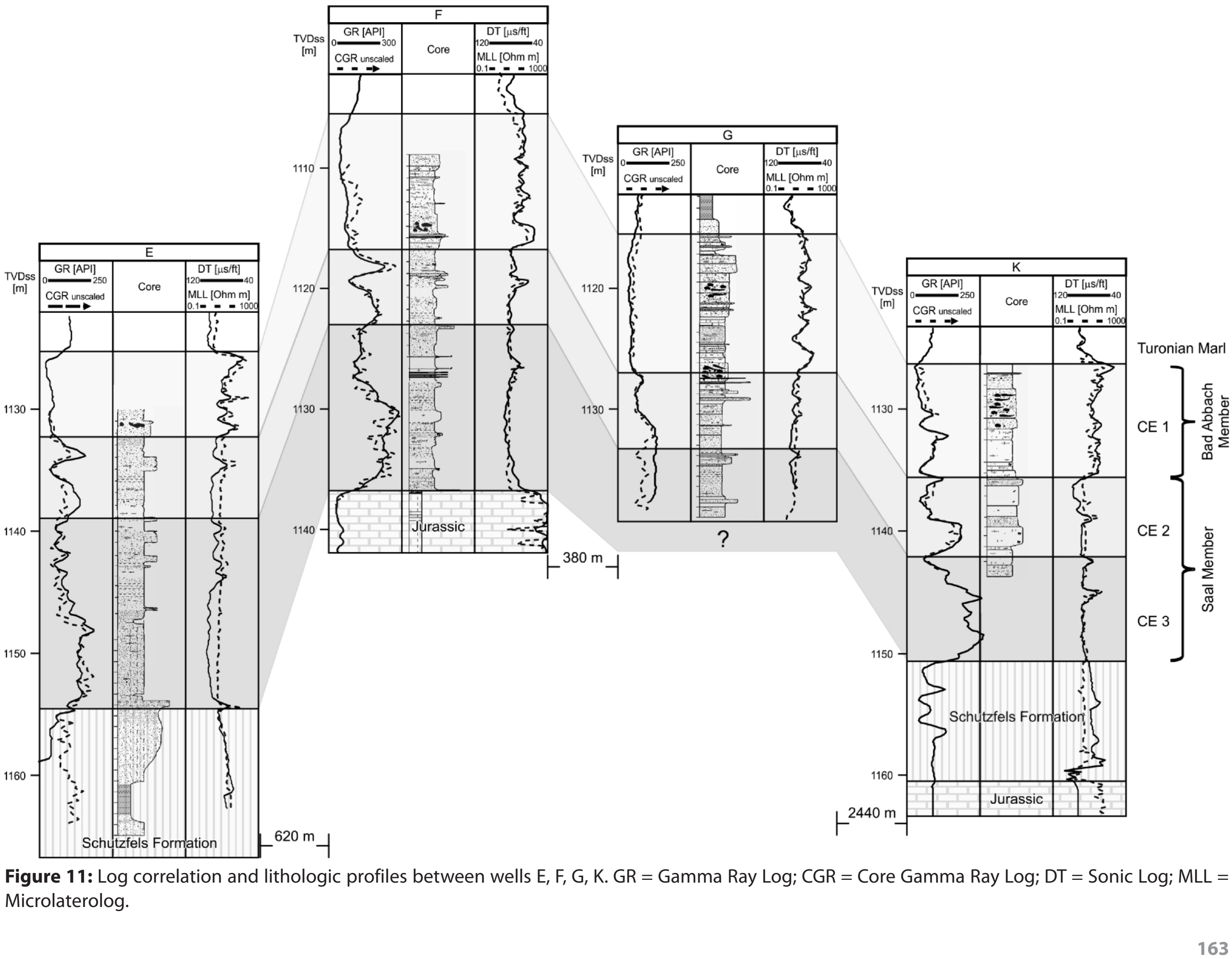

Figure 11: Log correlation and lithologic profiles between wells E, F, G, K. GR = Gamma Ray Log; CGR = Core Gamma Ray Log; DT = Sonic Log; MLL = Microlaterolog.

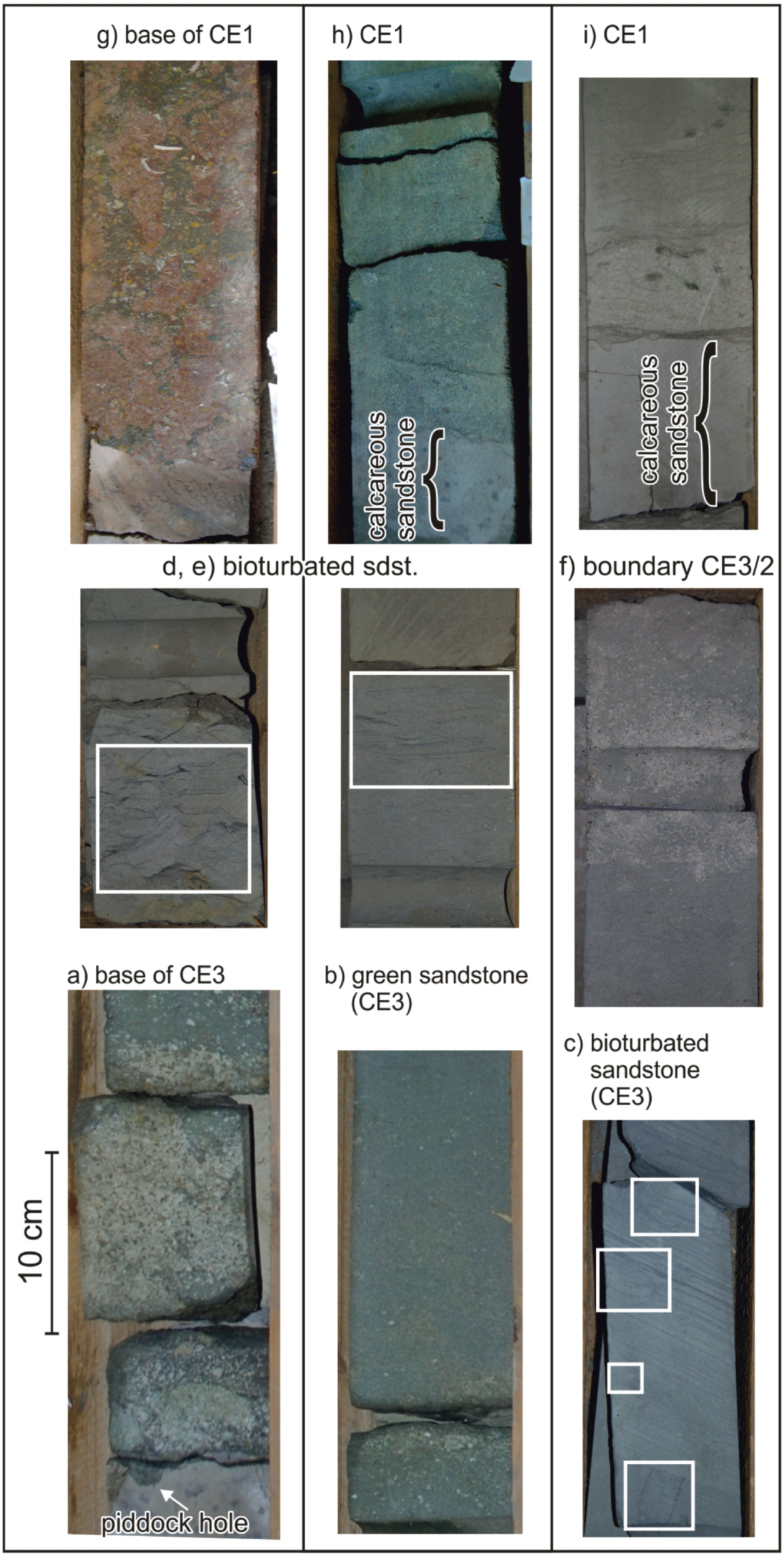

Figure 12: Core photographs. With the exception of c) (well E), all photographs are from well F. a) Conglomeratic base of CE3 overlying Malmian carbonate. b) Fine grained sandstone of CE3. c) CE3 sandstone with weak bioturbation (see white rectangles) d,e) Vertical and horizontal burrows in units CE3 and CE2 and cross bedding (e)). f) Bioturbated sandstone with bimodal grain size distribution (boundary CE3/2) g) Red "marker bed" (Nachtmann, 1995) at base of CE1. h) Green sandstone overlying thin layer of calcareous sandstone. i) Hardground separating calcareous from non-calcareous sandstone.

5. The Trattnach Field

5.1 History of the Trattnach Field

The Trattnach Field (Fig. 3) was discovered in 1975. Till 1980 nine wells were drilled and seven of them were used for production. The next well, a horizontal well, was drilled after 30 years of production in 2012. At present three wells are in production. The small Trattnach North Field was detected in 1983. It produced from Cenomanian sandstones till 1998.

The Trattnach and Trattnach North fields are the only fields in Upper Austria, which produce exclusively from Cenomanian layers. Eocene sandstones were dry in both fields.

5.2 Field Structure

The Trattnach Field is located in an anticlinal dome structure with shallow dipping flanks. Its western boundary is formed by the transpressional Schwanenstadt fault system. Consequently, well E which drilled the reservoir horizon within the Schwanenstadt fault system, was dry. The crest of the dome is at about 1090 m TVDss (True Vertical Depth sub sea). The initial oil-water-contact was defined at 1150 m depth TVDss.

The formation of the Trattnach anticlinal dome is linked to the

Paleocene compressive deformation phase. The isochron map of the Cretaceous sediments (Fig. 9d) provides an excellent presentation for the structure of the dome at the onset of Eocene sedimentation. The Aistersheim and the Gaspoltshofen fault systems displaced the Trattnach anticlinal dome in Oligo-/Miocene time, but do not contribute to the Trattnach trap. In contrast, the small Trattnach North Field is formed by an anticlinal structure sealed towards the north by the Aistersheim fault systems. The crest of this structure is at about 1135 m TVDss, its initial OWC was at ~1150 m TVDss.

A fault with minor displacement is located within the depression separating the Trattnach and Trattnach North fields (a in Fig. 10a). Its existence has been postulated based on pressure behavior, but is now well visible in the 3D seismic data.

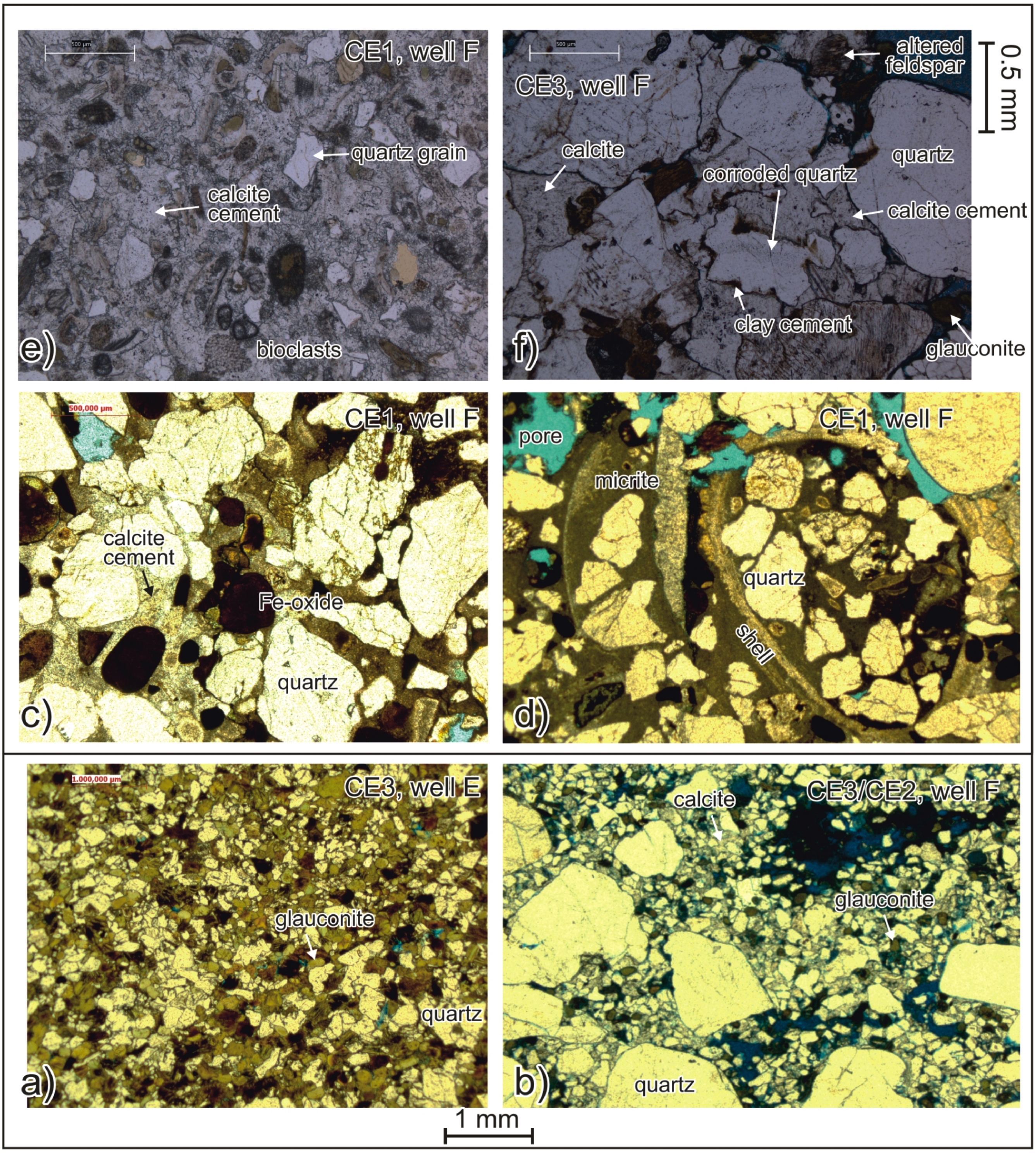

Figure 13: Thin section photographs of sandstones in the Regensburg Formation. With the exception of a) (well E), all microphotographs are from well F. a) Glauconitic fine-grained sandstone. b) Calcite cemented sandstone with bimodal grain size distribution (boundary between units CE3 and CE2; see Fig. 12f). c,d) red "marker bed" (see Fig. 12g). e,f) calcareous sandstone with bioclasts (see Figs. 12h,i).

5.3 Reservoir Description

The Trattnach and Trattnach North fields produce from Cenomanian layers. As mentioned earlier, the GR log in the Regensburg Formation is strongly influenced by Th contents in heavy minerals. K contents in glauconite play a secondary role (Fig. 7). Consequently, the GR log is a poor tool to determine shale contents. Therefore, DT and resistivity (e.g. microlaterolog, MLL) logs are used as correlation logs.

Nachtmann (1995) subdivided the Cenomanian into three units based on lithology and wireline logs. The lower units CE3 and CE2, composed of bioturbated fine- to medium-grained sandstones, represent the main reservoir layers. A calcareous sandstone layer which shows a distinct peak in the MLL log forms the boundary between CE3 and CE2. The base of the upper unit CE1 is formed by a red "marker bed" with high resistivity (Fig. 11) and consists mainly of calcareous, fossil-rich sandstone with very low permeability.

Based on higher carbonate contents in CE1, this unit is tentatively correlated with the Bad Abbach Member of the Regensburg Formation, where CE3 and CE2 are correlated with the Saal Member (Niebuhr et al., 2009; Wilmsen et al., 2010).

5.3.1 Depositional environment

CE3 and CE2 (equivalent of the Saal Mb): The base of the Cenomanian sandstone in the Trattnach Field is often characterized by a transgressive conglomerate (Fig. 6a, 12a). The bulk of the lithologically similar units CE3 and CE2 is formed by green fine-grained sandstone (Fig. 12b) with some layers of siltstone, medium- and coarse-grained sandstone. The greenish rock color originates from glauconite which often appears as pellets in different states of alteration (Fig. 13a), but also as cement. Apart from glauconite, the main minerals are quartz, potassium feldspar, illite/mica, chlorite and mixed layer clay minerals. Kaolinite is present in siginificant amounts in some samples. Calcite, dolomite and berthierine are typically rare. Macrofossils are largely missing, but foraminifera and sporadic ostracods occur within the green sandstones (Nachtmann, 1995). Calcite and minor dolomite form cement.

Primary sedimentary structures, like hummocky cross-stratification, are frequently destroyed by bioturbation (Fig. 12b,c). Both, horizontal and vertical burrows occur within these units (Fig. 12c,d,e). Burrows in fine grained sandstones are often filled with coarse grains. Mixing of both fractions results in bimodal grain size distributions (Fig. 13b). Coarser grains may originate from storm events. The ichnofacies indicates a shallow marine environment (upper/middle to lower shoreface).

A thin well cemented coarse-grained sandstone (Figs. 12f, 13b) with high resistivity and low DT-values forms a marker horizon and has been defined as the boundary between CE3 and CE2 (Nachtmann, 1995).

In general, there are only small differences between CE3 and CE2. In some wells the portion of the fraction with bigger grain sizes increases upwards.

CE1 (equivalent of the Bad Abbach Mb.): CE1 mainly consists of fossil-rich, bioturbated, often well cemented (calcareous) sandstones and conglomerates.

The base of CE1 is characterized by a "marker bed" (Nachtmann, 1995; Fig. 12g). Sediments of this 1 to 2 m thick layer consist of subrounded calcareous sandstone pebbles with reddish colors and sometimes a distinct red rim, calcareous fossil remains and a greenish (glauconitic) sandstone matrix. The sandstones mainly comprise quartz, calcite (cement), illite/mica, kaolinite, glauconite, berthierine and goethite, which is responsible for the reddish color (Fig. 13c,d). The "marker bed" is interpreted as terrestrial debris flows which were mixed with shallow marine sediments.

Similar to CE3 and CE2, sandstones often show a bimodal grain size distribution (Fig. 12h). Some grains are up to 1 cm in diameter. Coarser material was transported by storm events. Sandstones consist of quartz, glauconite, and calcite. In addition, berthierine, dolomite, kaolinite, illite and rare mixed layer minerals occur. Moreover, some sandstones layers are rich in clay minerals and show a matrix-supported fabric.

A unique feature of CE1 is the presence of calcareous sandstones, often with a hardground on top (e.g. lower part of Fig 12h,i). Calcareous sandstones contain high percentages of

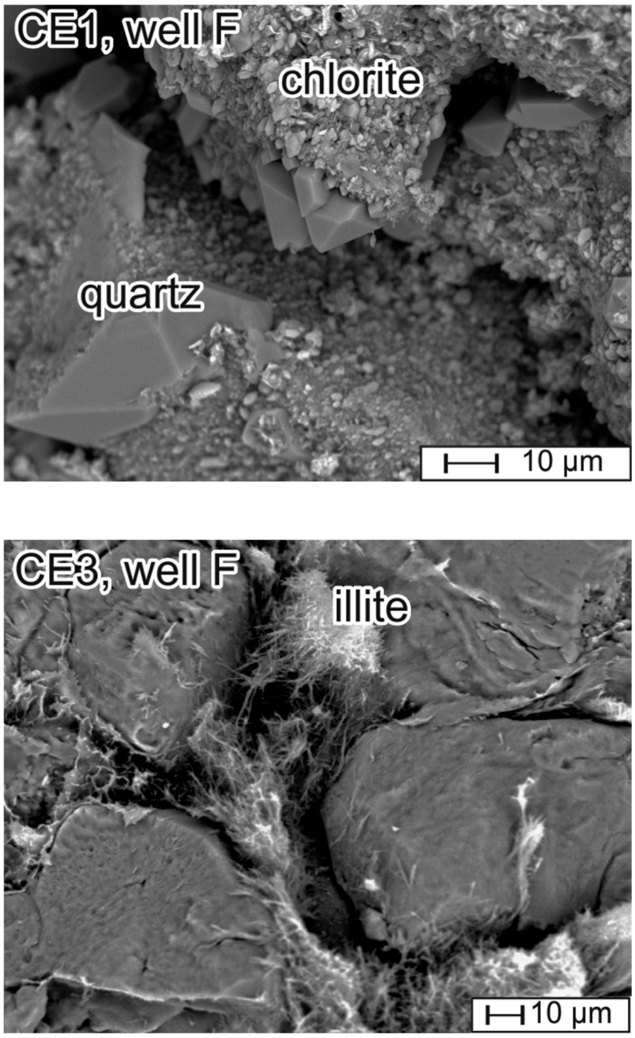

Figure 14: SEM photographs showing different cement types in sandstones from the Regensburg Formation.

bioclasts and (partly re-crystallized) limy mud (Fig. 13e). The siliciclastic fraction is formed by quartz, minor feldspar, glauconite, and sparse kaolinite. These bioclast rich calcareous sandstones are interpreted as sediments derived from low-energy debris flows. The regional geological setting suggests a transport direction from NE.

The ichnofacies point to a slight upward increase in water depth, which finally resulted in the deposition of calcareous shales representing deeper shelf facies (Eibrunn Fm., see also Wilmsen et al., 2010). Wilmsen et al. (2010) relate the transgressive development to a significant sea level rise.

5.3.2 Post-depositional diagenesis

The diagenetic history provides a significant contribution to the understanding of the reservoir quality. In general, a clayey primary matrix which reduces pore space significantly is typical for fine grained sandstones. Clay minerals from this matrix are often re-crystallized into chlorite. Sandstones, directly overlying Jurassic carbonates, show significant cementation with calcite followed by dolomite. Apart from its base, cementation in units CE3 and CE2 is generally weak, but locally small amounts of blocky and micritic calcite cement may occur (e. g. Fig. 13b).

Thin section analysis shows sparse quartz cement overgrowing detrital quartz grains during early diagenesis. Authigenic quartz is also visible in SEM pictures (Fig. 14a).

In comparison to CE3 and CE2, CE1 shows a significant higher amount of carbonate cement. Often two generations of blocky cement, an earlier one with smaller crystals and a later one with larger crystals, can be distinguished. It is suggested, that the higher carbonate content results from the presence of calcareous bioclasts and recrystallized limy mud. A high amount of carbonate cementation reduces porosity remarkable. However, the amount of cementation varies significantly in vertical direction. Furthermore, calcite concretions and larger pyrite nodules (~0.5 cm) are visible in cores of the Trattnach area.

Feldspar grains are often dissolved and altered into clay minerals (kaolinite) or replaced by calcite cement. Replacement of biotite by glauconite and of glauconite pellets by calcite can also be observed. Quartz grains are frequently corroded and overgrown by blocky calcite cement. Locally clay mineral cement coating the grains may be present between the quartz grains and the calcite cement (Fig. 13f). Occasionally blocky calcite cement replaced former clay mineral matrix (e.g. in the red "marker bed"). Sparse small pyrite formed after calcite ce-

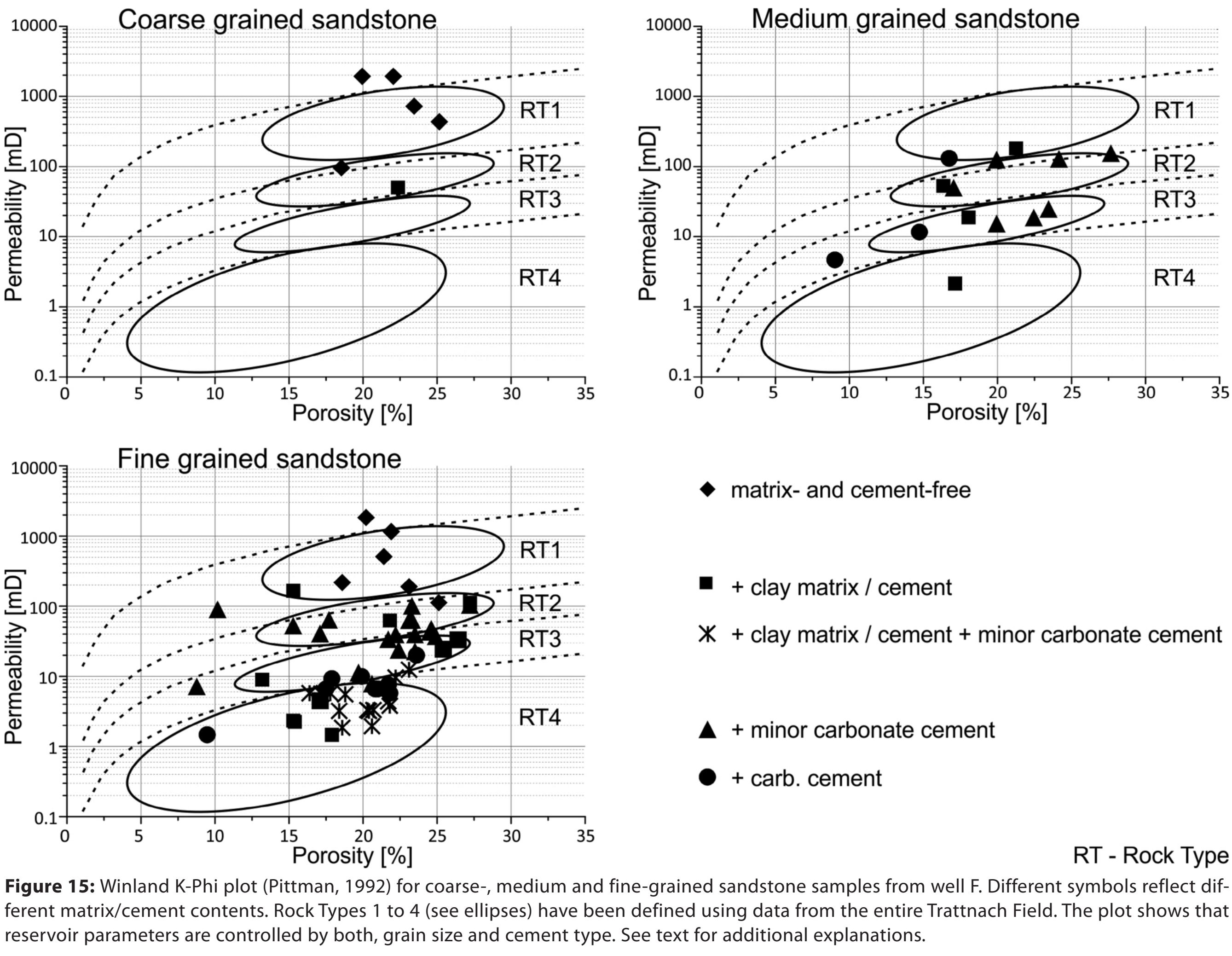

Figure 15: Winland K-Phi plot (Pittman, 1992) for coarse-, medium and fine-grained sandstone samples from well F. Different symbols reflect different matrix/cement contents. Rock Types 1 to 4 (see ellipses) have been defined using data from the entire Trattnach Field. The plot shows that reservoir parameters are controlled by both, grain size and cement type. See text for additional explanations.

mentation. In CE3/2 calcite and clay mineral cement are partially dissolved forming secondary porosity. Chlorite and illite were formed during late diagenesis (Fig. 14b), but before Miocene oil accumulation.

5.4 Reservoir fluids

Formation water in the Trattnach Field is characterized by low salinities. This and isotopically light water indicate a hydraulic connection with low-mineralized water of meteoric origin within Jurassic carbonate rocks (Andrews et al., 1987).

The Trattnach oil is a low-sulfur, light to medium oil with a density of 0.876 g/cm^3 and an API value of ~30°. The oil is slightly heavier than other Molasse oils from the same depth. Although there is no chemical evidence for biodegradation (e.g. loss of n-alkanes), the slightly enhanced API might indicate mild in-reservoir alteration (Gratzer et al., 2011), perhaps related to the meteoric water.

The Trattnach Field is located in the border region between fields with eastern and western oil families (see Gratzer et al., 2011). Isotope and biomarker data show that the Trattnach oil combines characteristics of oil from the western family (e.g. low C_{28}/C_{29} ratio, relatively high $\delta^{13}C$ values) and from the eastern family (e.g. low dibenzothiophene/ phenanthrene ratios). Biomarker ratios indicate the oil was generated at relatively high maturity (~0.9 %Rr; Gratzer et al., 2011). This is an evidence for long-distance (~50 km) lateral hydrocarbon migration.

The Trattnach oil is undersaturated with respect to gas (gas oil ration: 5 m^3/m^3). The Trattnach gas is wet (C1/[C2+C3] = <50), typical for associated thermal gas, methane is isotopi-cally very light ($\delta^{13}C$ ~ -70) typical for microbial gas. Reischenbacher and Sachsenhofer (2011) speculate that the isotope ratio indicates the presence of secondary microbial gas formed by the incipient biodegradation of oil. Alternatively, the very negative $\delta^{13}C$ values may indicate the mixing of pre-existing primary microbial gas with a later thermogenic hydrocarbon charge (see Milkov, 2011 for definitions of primary and secondary microbial gas).

5.5 Petrophysics

Petrophysical properties were used for reservoir characterization. A summary of these data was published by Nachtmann (1995). According to this paper, porosity values vary between 8 and 26 %. Permeability values range from <1 md to more than 3000 mD, but are typically in the order of few tens to few hundreds of mD (Fig. 15). 10 mD are accepted as threshold value distinguishing between reservoir and non-reservoir rocks. Capillary pressure curves suggest high initial water saturation (52 %). The recovery factor is at maximum 30 % in layers with high permeability. With decreasing permeability the recovery factor is decreasing below 10 %.

Rock Types were established by RAG using a Winland K-Phi plot (Pittman, 1992) and all available porosity and permeability values of the Trattnach Field (Fig. 15). Rock types 1 to 4 classify rocks with decreasing reservoir quality. Based on the permeability-cut-off value of 10 mD, rock type 4 is not considered as a reservoir rock.

As stated in section 5.3.2, apart from intergranular porosity, three different pore types can be recognized in Cenomanian reservoir sandstones. Intergranular porosity exists between grains, microporosity is associated with detrital and authigenic clay minerals, and porosity caused by dissolution of grains. The secondary porosity is largely destroyed by calcite and minor clay mineral cement.

To study the effect of grain size and the presence of matrix and cement, data from rock samples from well F with different grain sizes and matrix/cement content are plotted in Fig. 15. The plot shows that permeability is strongly controlled by grain size.

The best reservoir properties (permeability >100 mD) are found in coarse grained sands from the upper part of unit CE3. However, some clean fine grained sands (CE3) can also be highly permeable. Intergranular porosity prevails in these matrix- and cement-free samples.

In medium grained sandstone porosity is mainly controlled by the degree of carbonate cementation. Fine grained sands with carbonate cement, which are frequent in CE1, and fine grained sands with high clay contents, often observed in the lower part of CE3, plot into the low quality rock type 3.

Whereas calcite cement significantly reduces both, porosity and permeability, clay mineral matrix/cement has a major negative effect on permeability, but only a moderate effect on porosity. This is because even minor amounts of clay mineral cement may block pore throats, and because of microporosity associated with detrital and authigenic clay minerals.

6. Conclusion

The Trattnach area is located at the northern slope of the Austrian sector of the North Alpine Foreland Basin. Here, sedimentation started during Jurassic time. An Upper Jurassic carbonate platform overlies siliciclastic rocks and is separated from Upper Cretaceous shelf sediments by a major unconformity. Along the Central Swell Zone (Fig. 1b) an angular unconformity exists between Jurassic and Cretaceous rocks. However in the Trattnach area the contact seems to be concordant.

Whitish non-marine sandstones of the Lower Cretaceous Schutzfels Formation filled karst structures. The base of the Cenomanian Regensburg Formation is formed by a transgressive conglomerate, whereas the main part of the formation is characterized by bioturbated green sandstone rich in glauconite. The upper part of the Regensburg Formation contains a red "marker" bed and layers with calcareous sandstone rich in bioclasts. The sediments of the Regensburg Formation are interpreted as tempestites and debrites and grade upwards into deeper shelfal calcareous shales (Eibrunn Fm.) with an early Turonian age. The Cenomanian to Lower Turonian succession reflects drowning of the southern European margin. It is uncertain, whether the oceanic anoxic event OAE2 occurred during accumulation of the Eibrunn Formation. In any case, it did not result in deposition of source rocks.

Mesozoic to Paleocene tectonic events include Early Cretaceous uplift, Turonian/Coniacian E-W compression, both related to Cretaceous opening of the N-Atlantic, and Paleocene NE-SW compression caused by the closure of the Penninic Ocean. The Paleocene NE-SW compressional event resulted in the formation of the Trattnach Mega-Anticline and transpressional reactivation of the NNW-SSE trending Schwanenstadt fault system, which is probably a late Variscan fault zone.

Cenozoic Molasse sediments overlie the Mesozoic succession with a major angular unconformity and start with Eocene clastic and carbonate rocks. Fine-grained rocks follow above the Eocene carbonates and suffered a major Lower Oligocene submarine erosive event visible in 3D seismic data. Another major unconformity separates the Oligo-/Miocene Lower and Upper Puchkirchen formations from the Hall Formation with an Eggenburgian age.

E-W trending normal faulting (Aistersheim and Gaspoltshofen fault systems) related to flexural down-bending is the main Cenozoic tectonic event. Both fault systems show a main S-dipping fault plane and a subordinate N-dipping fault plane and were activated during earliest Oligocene time. Fault activity decreased during Egerian time and ended before the Eggenburgian. Seismic data show that the fault block confined by the Aistersheim and Gaspoltshofen faults was tilted during Late Oligocene (early Egerian) time.

The Trattnach Field, which came on stream during the mid-1970s, is located within the Trattnach Anticlinal Dome. Its western boundary is formed by the Schwanenstadt fault system. The Trattnach Field produces oil from the lower part of the Cenomanian green sandstones (CE3 and CE2). GR logs of the green sandstones are mainly controlled by Th contents and, therefore, should not be used for the distinction between shale and sand. Clay mineral, quartz and dominant carbonate cement can be distinguished. The reservoir quality (porosity, permeability) is controlled by grain size, sorting (presence of clay matrix), clay mineral and carbonate cement. The seal is formed by tight Cenomanian rocks (CE1) and Turonian shaly marls.

Formation water with low salinity indicates a hydraulic connection with meteoric water within Jurassic carbonate rocks (Andrews et al., 1987). The oil is low in sulfur and undersaturated with respect to gas. Oil accumulation commenced during Miocene time. Methane was formed by microbial activity.

Acknowledgments

The authors thank Rohöl-Aufsuchungs AG (RAG) for providing core material, well logs, seismic data. We also thank employees of RAG including Alan Reingruber, Werner Tschelaut, Hans-Gert Linzer, Mile Dragosavac, and the former employee Wolfgang Nachtmann, as well as Susanne Gier from University of Vienna for fruitful discussion. The authors wish to thank Schlumberger for providing academic license of the Petrel® software. Finally, we would like to thank the reviewers Birgit Niebuhr and Wolfgang Schollnberger for their constructive criticism and fruitful comments.

References

Andrews, J.N., Youngman, M.J., Goldbrunner, J.E. and Darling, W.G., 1987. The geochemistry of formation waters in the Molasse Basin of Upper Austria. Environmental Geology and Water Sciences, 10, 43-57.

Bachmann, G. H., Müller, M. and Weggen., K., 1987. Evolution of the Molasse Basin (Germany, Switzerland). Tectonophysics, 137, 77-92.

Bechtel, A., Gratzer, R., Linzer, H.-G. and Sachsenhofer, R. F., 2013. Influence of migration distance, maturity and facies on the stable isotopic composition of alkanes and on carbazole distributions in oils and source rocks of the Alpine Foreland Basin of Austria. Organic Geochemistry, 62, 74-85. http://dx.doi.org/10.1016/j.orggeochem.2013.07.008

Borowski, K., 2007. Lithofacies and depositional environment of the Upper Hall Formation, Alpine Molasse Basin, Upper Austria. Unpubl. Report, TU Bergakademie Freiberg, 126 pp.

Brix, F. and Schultz, O., 1993. Erdöl und Erdgas in Österreich. Veröffentlichungen aus dem Naturhistorischen Museum Wien, 688 pp.

Bradley, D.C. and Kidd, W.S.F., 1991. Flexural extension of upper continetal crust in collisional foredeeps. Geological Society of America, Bulletin, 113/11, 1416-1438.

Brandmayr, M., Dallmeyer, R.D., Handler, R. and Wallbrecher, E., 1995. Conjugate shear zones in the Southern Bohemian Massif (Austria): implications for Variscan and Alpine tectonothermal activity. Tectonophysics, 248, 97-116.

Butler, R.W., 1982. The terminology of structures in thrust belts. Journal of Structural Geology, 239-245.

Cox, T. and Seitz, K., 2007. Ant tracking seismic volumes for automated fault interpretation. CSPG/CSPE GeoConvention 2007, Calgary, Canada.

Dèzes, P., Schmid, S.M. and Ziegler, P.A., 2004. Evolution of the European Cenozoic Rift System: interaction of the Alpine and Pyrenean orogens with their foreland lithosphere. Tectonophysics, 389, 1-33. http://dx.doi.org/10.1016/j.tecto.2004.06.011

De Ruig, M.J., 2003. Deep Marine Sedimentation and Gas Reservoir Distribution in Upper Austria. OIL GAS European Magazine, 64-73.

De Ruig, M.J. and Hubbard, S.M., 2006. Seismic facies and reservoir characteristics of a deep-marine channel belt in the Molasse forelnad basin, Puchkirchen Formation, Austria. AAPG Bulletin, 90, 735-752. http://dx.doi.org/10.1306/10210505018

Genser, J., Cloething, S.A.P.L. and Neubauer, F., 2007. Late orogenic rebound and oblique Alpine convergence: New constraints from subsidence analysis of the Austrian Molasse basin. Global and Planetary Change, 214-223. http://dx.doi.org/10.1016/j.gloplacha.2007.03.010

Gratzer, R., Bechtel, A., Sachsenhofer, R.F., Linzer, H.-G., Reischenbacher, D. and Schulz, H.-M., 2011. Oil-oil and oil-source rock correlations in the Alpine Foreland Basin of Austria: Insights from biomarker and stable carbon isotope studies. Marine and Petroleum Geology, 28, 1171-1186. http://dx.doi.org/10.1016/j.marpetgeo.2011.03.001

Grunert, P., Hinsch, R., Sachsenhofer, R.F., Bechtel, A., Ćorić, S., Harzhauser, M., Piller, W.E. and Sperl, H., 2013. Early Burdigalian infill of the Puchkirchen Trough (North Alpine Foreland Basin, Central Paratethys): Facies development and sequence stratigraphy. Marine and Petroleum Geology, 39, 164-186. http://dx.doi.org/10.1016/j.marpetgeo.2012.08.009

Grunert, P., Auer, G., Harzhauser, M. and Piller, W. E., 2015. Stratigraphic constraints for the upper Oligocene to lower Miocene Puchkirchen Group (North Alpine Foreland Basin, Central Paratethys). Newsletters on Stratigraphy, 48/1, 111-133. http://dx.doi.org/10.1016/j.tecto.2004.06.011

Gusterhuber, J., Dunkl, I., Hinsch, R., Linzer, H.-G. and Sachsenhofer, R.F., 2012. Neogene Uplift and Erosion in the Alpine Foreland Basin (Upper Austria and Salzburg). Geologica Carpathica, 63, 4, 295-305. http://dx.doi.org/10.2478/v10096-012-0023-5

Gusterhuber, J., Hinsch, R., Linzer, H.-G. and Sachsenhofer, R. F., 2013. Hydrocarbon generation and migration from subthrust source rocks to foreland reservoirs: The Austrian Molasse Basin. Austrian Journal of Earth Scienes, 106/2, 115-136.

Gusterhuber, J., Hinsch, R. and Sachsenhofer, R.F., 2014. Evaluation of hydrocarbon generation and migration in the Molasse fold and thrust belt (Central Eastern Alps, Austria), using structural and thermal basin models. AAPG Bulletin, 98, 2, 253–277. http://dx.doi.org/10.1306/06061312206

Kröll, A., Wagner, L., Wessely, G. and Zych, D., 2005. Molassezone Salzburg-Oberösterreich. Strukturkarte der Molassebasis 1:200 000. Geologische Bundesanstalt, Vienna.

Linzer, H.-G. and Sachsenhofer, R.F., 2010. Submarine Large Scale Mass Movements in the Deepwater Foreland Basin of the Alps - Implications to Hydrocarbon Generation and Distribution of Source and Reservoir Rocks. AAPG Search and Discover Article #90104©2010 AAPG Annual Convention and Exhibition, 11-14 April 2010.

Malzer, O., Rögl, F., Seifert, P., Wagner, L., Wessely, G. and Brix, F., 1993. Die Molassezone und deren Untergrund. In: F. Brix and O. Schulz (eds.), Erdöl und Erdgas in Österreich. Veröffentlichungen aus dem Naturhistorischen Museum Wien, 281-358.

Nachtmann, W., 1995. Das Cenoman im Untergrund der oberösterreichischen Molasse – eine lagerstättengeologische Betrachtung. Zentralblatt für Paläontologie, Teil I, 1/2, 271-281.

Nachtmann, W. and Wagner, L., 1987. Mesozoic and Early Tertiary evolution of the Alpine foreland in Upper Austria and Salzburg, Austria. Tectonophysics, 137, 61-76.

Niebuhr, B., Pürner, T. and Wilmsen, M., 2009. Lithostratigraphie der außeralpinen Kreide Bayerns. Schriftenreihe der Deutschen Gesellschaft für Geowissenschaften, 65, 7-58.

Niebuhr, B., Wilmsen, M., Chellouche, P., Richardt, N. and Purner, T., 2011. Stratigraphy and facies of the Turonian (Upper Cretaceous) Roding Formation at the southwestern margin of the Bohemian Massif (Southern Germany, Bavaria). Zeitschrift der Deutschen Gesellschaft für Geowissenschaften, 162, 295-316. http://dx.doi.org/10.1127/1860-1804/2011/0162-0295

Niebuhr, B., Wilmsen, M. and Janetschke, N., 2014. Cenomanian–Turonian sequence stratigraphy and facies development of the Danubian Cretaceous Group (Bavaria, Southern Germany). Zeitschrift der Deutschen Gesellschaft für Geowissenschaften, 165, 621-640. http://dx.doi.org/10.1127/zdgg/2014/0022

Oschmann, F., 1958. Erläuterungen zur geologischen Karte von Bayern 1 : 25.000, Blatt Nr. 7038, Bad Abbach. Bayerisch. Geol. Landesamt, München, 184 pp.

Peters, K.E., 1986. Guidelines for Evaluating Petroleum Source Rock Using Programmed Pyrolysis. AAPG Bulletin, 70, 318-329.

Pederson, S.I., Randen, T., Sonneland, L. and Stehen, O., 2002. Automatic 3D fault interpretation by artificial ants. 72nd Annual International Meeting, SEG, Expanded Abstracts, 512-515.

Pittman, E.D., 1992. Relationship of porosity to permeability to various parameters derived from mercury injection-capillary pressure curves for sandstone. AAPG Bulletin, 76, 191-198.

Rasser, M.W. and Piller, W.E., 2004. Crustose algal frameworks from the Eocene Alpine Foreland. Palaeogeography, Palaeoclimatology, Palaeoecology, 206, 21-39. http://dx.doi.org/10.1016/j.palaeo.2003.12.018

Reischenbacher, D. and Sachsenhofer, R.F., 2011. Entstehung von Erdgas in der oberösterreichischen Molassezone: Daten und offene Fragen. Berg- und Hüttenmännische Monatshefte, 156/11, 455-460. http://dx.doi.org/10.1007/s00501-011-0037-9

Sachsenhofer, R.F. and Schulz, H.-M., 2006. Architecture of Lower Oligocene source rocks in the Alpine Foreland Basin: a model for syn- and post-depositional source-rock features in the Paratethyan realm. Petroleum Geoscience, 12, 363-377. http://dx.doi.org/10.1144/1354-079306-712

Sachsenhofer, R.F., Leitner B., Linzer H.-G., Bechtel A., Coric, S., Gratzer, R., Reischenbacher, D. and Soliman, A., 2010. Deposition, erosion and hydrocarbon source potential of the Oligocene Eggerding Formation (Molasse Basin, Austria). Austrian Journal of Earth Sciences, 103/1, 76-99.

Schlanger, S.O., Arthur, M.A., Jenkyns, H.C. and Scholle, P.A., 1987. The Cenomanian-Turonian oceanic anoxic event: I. Stratigraphy and distribution of organic-rich beds and the marine $\delta^{13}C$ excursion. In: J. Brooks and A.J. Fleet (eds.), Marine and Petroleum Source Rocks. Geological Society London, Special Publications, 26, 371-399.

Schmidt, F. and Erdogan, L.T., 1996. Paleohydrodynamics in exploration. In: G. Wessely and W. Liebl (eds.), Oil and Gas in Alpidic Thrust belts and Basins of Central and Eastern Europe. EAGE Special Publication, 5, 255-265.

Schulz, H.-M., Sachsenhofer, R.F., Bechtel, A., Polesny, H. and Wagner, L., 2002. The origin of hydrocarbon source rocks in the Austrian Molasse Basin (Eocene - Oligocene transition). Marine and Petroleum Geology, 19/6, 683-709. http://dx.doi.org/10.1016/S0264-8172(02)00054-5

Schulz, H.-M., Bechtel, A. and Sachsenhofer, R.F., 2005. The birth of the Paratethys during the early Oligocene: from Tethys to an ancient Black Sea analogue? Global and Planetary Change, 49, 163-176. http://dx.doi.org/10.1016/j.gloplacha.2005.07.001

Sissingh, W., 1997. Tectonostratigraphy of the North Alpine Foreland Basin: correlation of Tertiary depositional cycles and orogenic phases. Tectonophysics, 282, 223-256. http://dx.doi.org/10.1016/S0040-1951(97)00221-7

Trusheim, F., 1935. Die geologische Geschichte Südostdeutschlands während der Unterkreide und des Cenomans. Neues Jahrbuch für Mineralogie, Geologie und Paläontologie, Beil., B 75, 1-109.

Véron, J. 2005. The Alpine Molasse Basin – Review of Petroleum Geology and Remaining Potential. Bulletin für angewandte Geologie, 10, 75-86.

von Hartmann, H., Buness, H., Krawczyk, C.M. and Schulz, R., 2012. 3-D seismic analysis of a carbonate platform in the Molasse Basin - reef distribution and internal separation with seismic attributes. Tectonophysics, 572-573, 16-25. http://dx.doi.org/10.1016/j.tecto.2012.06.033

Wagner, L.R., 1996. Stratigraphy and hydrocarbons in the Upper Austrian Molasse Foredeep (active margin). In: G. Wessely and W. Liebl (eds.), Oil and Gas in Aplidic Thrustbelts and Basins of Central and Eastern Europe. EAGE Special Publications, 5, 217-235.

Wagner, L.R., 1998. Tectono-stratigraphy and hydrocarbons in the Molasse Foredeep of Salzburg, upper and lower Austria. In: Mascle, A., Puigdefabregas, C., and Luterbach, H.P. (eds.), Cenozoic Foreland Basins of Western Europe. Geological Society London, Special Publications, 134, 339-369.

Wilmsen, M., Niebuhr, B., Chellouche, P., Pürner, T. and Kling, M., 2010. Facies pattern and sea-level dynamics of the early Late Cretaceous transgression: a case study from the lower Danubian Cretaceous Group (Bavaria, southern Germany). Facies, 56, 4, 483-507. http://dx.doi.org/10.1007/s10347-010-0224-2

Ziegler, P.A., 1987. Late Cretaceous and Cenzoic intra-plate compressional deformation in the Alpine foreland - a geodynamic model. Tectonophysics, 137, 389-420.

Received: 17 November 2014
Accepted: 17 August 2015

Doris GROSS[1)*)], Reinhard SACHSENHOFER[1)], Arno RECH[1)3)], Stefan SAGEDER[1)4)], Martin GEISSLER[1)2)], Stephan SCHNITZER[1)5)] & Wilma TROISS[2)]

[1)] Chair of Petroleum Geology, Department Applied Geosciences and Geophysics, Montanuniversität Leoben, Peter-Tunner-Strasse 5, 8700 Leoben, Austria;

[2)] Rohöl-Aufsuchungs AG, Schwarzenbergplatz 16, 1015 Wien, Austria;

[3)] OMV AG, 2230 Gänserndorf, Austria;

[4)] Total E&P, 64018 Pau, France;

[5)] GDF SUEZ E&P Deutschland GmbH, Waldstraße 39, 49803 Lingen, Germany;

[*)] Corresponding author, thomas.neubauer@nhm-wien.ac.at